To the Graduate Council:

I am submitting herewith a thesis written by Sunil Abraham entitled "Effect of Surface Defects on the Nucleation of CVD Diamond on 6H Silicon Carbide". I have examined the final copy of this thesis for form and content and recommend that it be accepted in partial fulfillment of the requirements for the degree of Master of Science, with a major in Metallurgical Engineering.

Carl J. McHargue, Major Professor

We have read this thesis
and recommend its acceptance:

R. A. Buchanan

T. T. Meek

Accepted for the council:

Associate Vice Chancellor
and Dean of The Graduate School

EFFECT OF SURFACE DEFECTS ON THE NUCLEATION OF CVD DIAMOND ON 6H SILICON CARBIDE

A Thesis

Presented for the

Master of Science

Degree

The University of Tennessee, Knoxville

Sunil Abraham

August 1994

ACKNOWLEDGMENTS

I wish to thank my major professor, Dr. C. J. McHargue, for his support and guidance throughout the course of this project. I also wish to thank Dr. R. A. Buchanan and Dr. T. T. Meek for their efforts as members of my thesis committee.

I am grateful to a number of people at Oak Ridge National Laboratory for their advice and assistance. In particular, I am indebted to Dr. R. E. Clausing for his patience and understanding during my work with diamond deposition. I am also grateful to Mr. Lee Heatherly for his invaluable help and suggestions concerning this study.

I would also like to thank Dr. John Hunn for his work in implantation of the substrates used in this study. Thanks are also due to Ms. Dorothy W. Coffey for her patience in training me to use the scanning electron microscope at HTML.

ABSTRACT

The thin SiC layer often observed between a Si substrate and a diamond film has led to the belief that the formation of this SiC layer precedes diamond nucleation . However, the nucleation of diamond on a clean, undamaged SiC surface is difficult .

Some of the defects introduced by abrading the surface of many substrate materials with diamond powder before deposition appear to serve as nucleation sites. Atomic scale defects (vacancies, interstitials) and impurities can be introduced by ion implantation. This thesis reports the effects of abrasion and ion-implantation on the nucleation of diamond on SiC during hot-filament assisted CVD.

Single crystal 6H SiC with the external face composed of Si or C were used as substrates. Silicon (150 keV) and C (55 keV) ion were implanted at fluences between 2 x 10^{14} / cm^2 and 2 x 10^{15} / cm^2 .

Nucleation did not occur on as-received or implanted samples. Abrasion with diamond powder using an ultra-sonic cleaner bath caused profuse nucleation on all samples. It was found that nucleation density on abraded samples decreased when implanted with increasing fluence of ions. Fluences of 2 x 10^{14} Si^+/cm^2 (150 keV) and 4x 10^{14} C^+/cm^2 (55 keV) did not effect the nucleation of diamond on silicon carbide. However, a fluence of 2 x 10^{15} Si^+/cm^2 completely suppresses the nucleation of diamond.

RBS / channeling studies on the high fluence implanted silicon carbide sample showed the presence of an amorphous layer at the surface, thereby

questioning some of the recently proposed theories about the mechanism of CVD diamond nucleation.

It is proposed that healing or smoothing of micro-flaws which are thought to act as nucleation sites, is an important mechanism to reduce the diamond nucleation density by ion implantation. Further work needs to be done to determine the exact nature of the mechanism by which ion implantation influences the nucleation of CVD diamond.

TABLE OF CONTENTS

CHAPTER		PAGE
1.	**INTRODUCTION**	1
2.	**LITERATURE REVIEW**	6
	2.1 Historical Introduction to Diamond Synthesis	6
	2.2 Low Pressure Synthesis	9
	2.3 Hot Filament CVD Diamond Deposition Process	10
	2.4 The Hot Filament Equipment	11
	2.4.1 Filament material	12
	2.4.2 Carburization	14
	2.5 Substrate Materials	15
	2.6 Nucleation of Diamond	17
	2.7 Methods of Surface Treatment for Nucleation Enhancement	17
	2.7.1 Scratching the substrate	18
	2.7.2 Covering the surface with carbon phases	20
	2.7.3 Interface chemistry	21
	2.8 Introduction to Ion Implantation	21
3.	**MOTIVATION FOR THIS WORK**	23
4.	**EXPERIMENTAL PROCEDURE**	25
	4.1 Substrate Treatments	25
	4.1.1 Polishing	25
	4.1.2 Ion implantation	25

4.2 Diamond Deposition 26
4.3 Scanning Electron Microscopy 30
5. RESULTS AND DISCUSSION 32
6. CONCLUSIONS 59
REFERENCES 61
APPENDIX 67
VITA 70

LIST OF FIGURES

FIGURE		PAGE
1.1	Potential CVD diamond applications	5
4.1	Schematic diagram of the experimental setup used for diamond deposition in this study	27
4.2	Design of a CVD chamber for diamond deposition can be very simple	28
5.1	Low magnification SEM micrograph showing diamond nucleation on a sample abraded with diamond powder in the ultrasonic vibrator	33
5.2	Higher magnification SEM micrograph showing same area as in fig. 5.1	34
5.3	SEM micrograph showing high diamond nucleation density on the non implanted surface of a Si faced sample	35
5.4	SEM micrograph showing diamond nucleation on implanted (2 x 10^{14} Si^{+} cm^{-2}, 150 keV) region of Si faced sample	36
5.5	SEM micrograph showing diamond nucleation on non implanted region of C faced sample	38
5.6	SEM micrograph showing diamond nucleation on implanted (2 x 10^{14} Si^{+} cm^{-2}, 150 keV) region of C faced sample	39

5.7 SEM micrograph showing diamond nucleation on implanted (4 x 10^{14} Si^+ cm^{-2}, 150 keV) region of Si faced sample..... 40

5.8 SEM micrograph showing diamond nucleation on non implanted region of the same Si faced sample as in fig. 5.7..... 41

5.9 SEM micrograph showing diamond nucleation on non implanted region of C faced sample..... 43

5.10 SEM micrograph showing diamond nucleation on implanted (4 x 10^{14} Si^+ cm^{-2}, 150 keV) region of aC faced sample..... 44

5.11 Difference in diamond nucleation between the non implanted and implanted regions (2 x 10^{15} Si^+ cm^{-2}, 150 keV) of Si faced sample..... 45

5.12 Difference in diamond nucleation between the non implanted and implanted regions (2 x 10^{15} Si^+ cm^{-2}, 150 keV) of C faced sample..... 46

5.13 SEM micrograph showing effect of Si implantation (2 x 10^{15} Si^+ cm^{-2}, 150 keV) followed by carbon implantation (4 x 10^{14} C^+ cm^{-2}, 55 keV) on a Si faced sample..... 47

5.14 SEM micrograph showing effect of Si implantation (2 x 10^{15} Si^+ cm^{-2}, 150 keV) followed by carbon implantation (4 x 10^{14} C^+ cm^{-2}, 55 keV) on a C faced sample..... 49

5.15 Effect of increasing fluence of Si implantation on the nucleation density of CVD diamond on Si faced 6H SiC..... 51

5.16 Effect of increasing fluence of Si implantation on the nucleation density of CVD diamond on C faced 6H SiC..... 52

5.17 Carbon faced SiC has lower nucleation density in comparison to Si faced SiC substrates..... 53

5.18 RBS/channeling of 6H SiC implanted with Si ions at 150 keV (2 x 10^{15} Si^+ cm^{-2}, 2 x 10^{14} Si^+ cm^{-2})..... 55

5.19 RBS/channeling of 6H SiC implanted with Si ions at 150 keV (4x 10^{14} Si^+ cm^{-2})..... 56

5.17 SEM micrograph showing diamond nucleation on the back side of a silicon faced sample..... 57

CHAPTER 1

INTRODUCTION

Diamond is the hardest known substance and the least compressible. It is a better conductor of heat at room temperature than any other material and, when free of impurities, one of the most transparent. Some of the typical property values of diamond are listed in Table 1.1. These properties can be traced to the material's unusual bonding: the atoms of a diamond crystal are more densely packed than those in any other known material. Furthermore, the forces that tie the atoms to one another are stronger than those in most solids. In addition to their scientific interest, such extreme properties make diamond technologically useful.

Diamonds have been valued as gemstones and noted for their hardness for at least two millennia but have only been available in relatively large numbers since about 1870 when extensive deposits were discovered in South Africa. One of the first known references to diamond is by the Roman writer Pliny (*circa* AD 70) who describes crystals apparently diamond, coming from India, presumably from alluvial river deposits. No sources of diamond outside India were known until the early eighteenth century when alluvial deposits were found in Brazil. The next stage in the diamond story came in 1897 when diamonds were found in alluvial deposits in South Africa near the Orange River. Mining of natural diamond still continues but it is rare and expensive.

Of all the problems tackled by mankind over the centuries, diamond synthesis ranks with the synthesis of gold as the Alchemists' ultimate dream. Economic gold synthesis is still in the realms of nuclear fiction whereas

Table 1.1 : Properties of diamond

Chemical Reactivity	Extremely Low
Density	3520 Kg m^{-3}
Hardness	9000 kg mm^{-2}
Heat Conductivity	20 w cm^{-1} $^{\circ}K^{-1}$ at 30 $^{\circ}C$
Tensile Strength	0.5 x 10^6 psi (natural)
Compressive Srength	14 x 10^6 psi (natural)
Thermal Expansion Coeff.	0.8 x 10^{-6} $^{\circ}K^{-1}$
Refractive Index	2.41 at 590 nm
Transmissivity	225 μm -far IR
Friction Coeffecient	0.05 (dry)
Band Gap	5.48 eV
Electrical Resistivity	10^{16} ohm-cm (natural)
Youngs Modulus	1050 GPa

diamond synthesis has been a commercial reality for the past 20 years. Of all the methods being used to produce synthetic diamond, chemical vapor deposition (CVD) is the most common because of its simplicity and inexpensive nature. At present, the interest in diamond films centres on three different areas of application, their use as hard protective coatings on tools and other devices, the possibility of constructing semiconducting electronic devices, and as a valuable adjunct to previous methods of growing diamonds under controlled conditions.

The coating of cutting tools with thin films of various hard materials is becoming increasingly common but none of these materials have the hardness of diamond. Therefore the possibility of coating say a tungsten carbide tool with a diamond film is most attractive as the diamond is very hard and the carbide is strong and tough. Therefore considerable attention is being paid to the problem of obtaining good adhesion between the film and the substrate. In general, the best adhesion between a film and its substrate is obtained when the film has grown epitaxially on the substrate, that is when the deposited atoms take sites correlated with the positions of the atoms in the substrate, and the lattice of the film has a particular orientation with respect to the substrate. For example, a diamond film will grow on the surface of a single crystal of diamond as a single crystal with the same orientation, without any loss of strength across the boundary. However, if the atoms in the substrate have arrangements and spacings much different from those in diamond it will be difficult to obtain epitaxial growth and the bond to the substrate will be considerably weaker. Besides the use of diamond films as protective coatings there has been extensive research and interest on their use as semi-conductor materials [1].

This interest derives from the possibility of growing films doped with boron so as to produce semi-conducting diamond. This application also requires the deposition of films with the high degree of crystal perfection necessary for the manufacture of useful devices.

The technique of growing diamond films by chemical vapor deposition offers the possibility of growing diamonds with more precise and controlled properties. CVD diamond films could be used in the high temperature - high pressure process to produce single crystal diamond particles larger in size compared to the starting film.

Other properties of CVD diamond films and their potential applications are listed in Figure 1.1.

It is clear from the above discussion that the growth of heteroepitaxial diamond film by chemical vapor deposition opens up considerable possibilities with numerous applications. One of the most important parameters influencing the heteroepitaxy of diamond on nondiamond substrates is the nucleation phenomena which in turn is a function of the substrate surface conditions. However, despite rapid progress, the mechanism(s) for diamond nucleation onto nondiamond substrates remains unknown. Several theories have been proposed based on specific cases but none of them can account for all the observations made so far.

This work aims at studying the effect of surface defects on the nucleation of CVD diamond. One goal of this research is to test some of the most recent theories of diamond nucleation. The use of ion-implantation as a surface modification tool and its influence on diamond nucleation are studied.

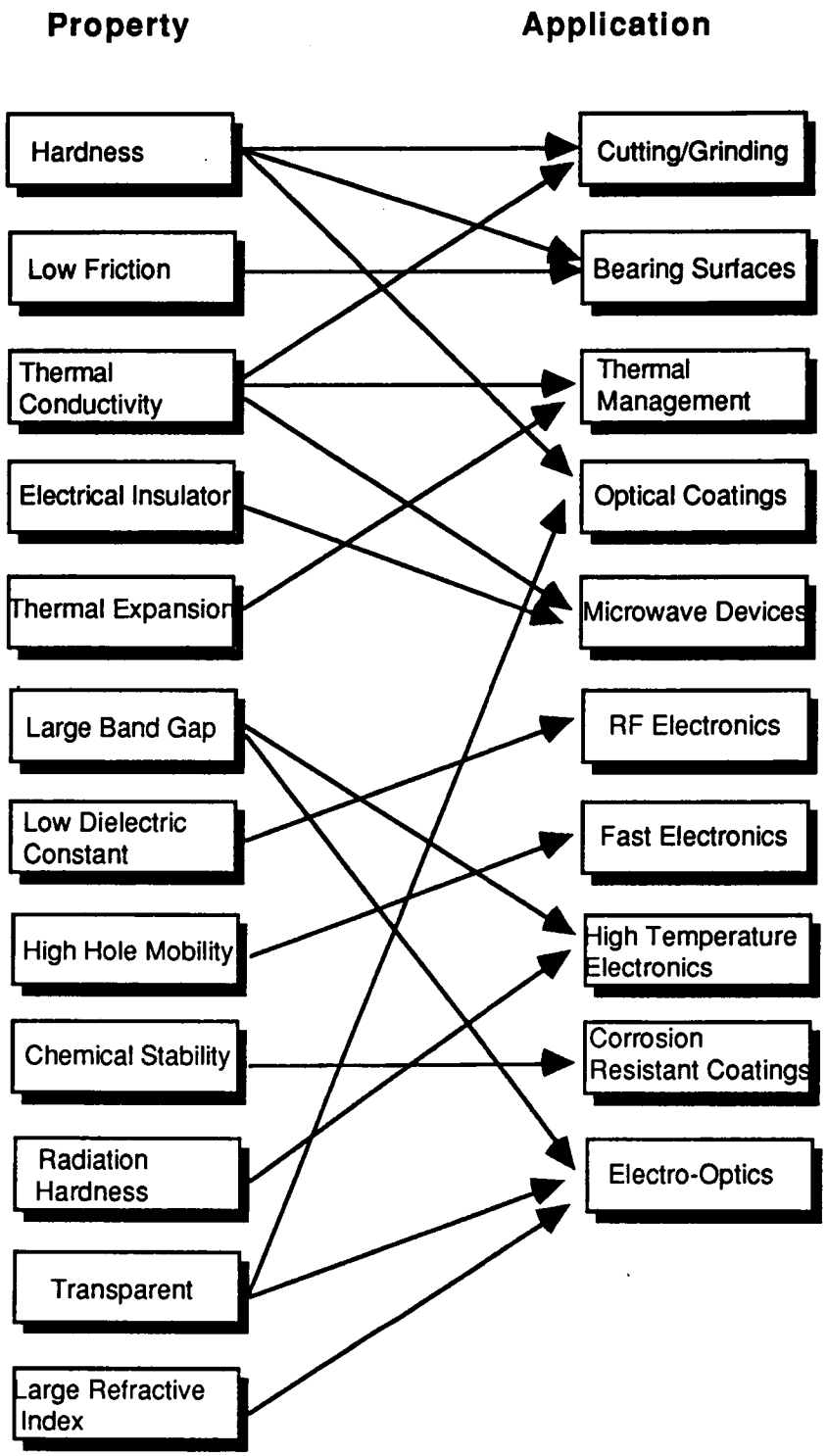


Figure 1.1: Potential CVD diamond applications [2].

CHAPTER 2

LITERATURE REVIEW

2.1 Historical Introduction to Diamond Synthesis

Diamond synthesis is the name given to the process whereby carbon (in some non-diamond form) is transformed into diamond. Of all the problems tackled by mankind over the centuries, diamond synthesis ranks with the synthesis of gold as the Alchemists' ultimate dream. Economic gold synthesis is still in the realms of nuclear fiction whereas diamond synthesis has been a commercial reality for the past 20 years. An extensive review of the history of diamond growth was provided by John Angus [3].

Ever since the late 18th century, when Antoine Laurent Lavoiser discovered that diamond is a crystalline form of carbon, laymen and scientists alike have tried to turn 'worthless' carbon into 'priceless' diamond. Initially, high pressures were used simply because diamond was the densest carbon phase. As understanding of chemical thermodynamics developed throughout the nineteenth and twentieth centuries, that intuitive notion was made quantitative and the pressure-temperature range of diamond stability was explored. These efforts culminated in the announcement in 1955 of a process for diamond synthesis using a molten transition metal solvent/catalyst at pressures where diamond is the thermodynamically stable phase [4]. Synthetic diamond made by high pressure processes is now a commonplace item of commerce.

A parallel effort directed towards the growth of diamond at low pressures where it is the metastable form of solid carbon has now reached the stage of commercial realization. The most successful process for low pressure growth of

diamond has been chemical vapor deposition from energetically activated hydrocarbon/hydrogen gas mixtures.

The first well documented report of diamond growth at low pressures, which was subsequently confirmed by others, was that of William G. Eversole at the Union Carbide Corporation [5]. He grew diamond seed crystals on pre-existing diamond seeds from carbon monoxide and hydrocarbon gases at moderate pressures. This predates the successful synthesis at high pressure by the General Electric team of Bundy , Hall, Strong and Wentorf [4].

Angus and co-workers at Case Western Reserve University were the first to confirm Eversole's results [6]. The Angus group first reported the use of atomic hydrogen, generated by a heated tungsten filament, for removing graphitic deposits and for rationalizing the diamond surface for future diamond growth [7]. They also observed sintering and restructuring of crystals heated under atomic hydrogen. Chauhan [8] and Fedoseev [9] showed that addition of molecular hydrogen to the hydrocarbon gas phase suppressed the growth rate of graphite more than it suppressed the growth rate of diamond, resulting in higher diamond yields.

The next confirmation of Eversole's work was obtained by the Soviet group at the Institute of Physical Chemistry in Moscow. Polycrystalline as well as single crystal films of diamond on single crystal diamond substrates were reported in the seventies by the Russian team of Spitsyn, Bouilov, Derjaguin, and coworkers by the gas chemical transport reaction method [10-12].

By the mid 1970's diamond growth at low pressures was achieved by several groups. The beneficial role of hydrogen was well known and understood to some extent. Although average linear growth rates were low, the

mass rate of diamond growth was quite high, even by today's standards, because very high surface area powders were used as substrates. Critical reviews of diamond synthesis published in this era accepted the conclusion that diamond could be grown at low pressures [13].

The increase in interest in metastable diamond growth can be traced to the discovery that the presence of atomic hydrogen during the growth process is essential to achieving high growth rates. Moreover, atomic hydrogen permits the de novo nucleation of new diamond crystallites on non-diamond substrates. This result was apparently first achieved by Soviet workers. The Soviet group mentions the use of atomic hydrogen during diamond growth, but does not describe the growth method [11]. These results received little attention, in part because the experimental method for growing the crystals was not revealed. Also, the association of the Derjaguin group with the polywater episode probably played a role in the skepticism with which these results were received.

The first descriptions of methods for rapid growth of diamond at low pressures were made by a group of Japanese researchers associated with the National Institute for Research in Inorganic Materials (NIRIM). They first achieved successful diamond synthesis using a hot filament to activate methane/hydrogen gas mixtures. A remarkable series of papers was presented by the NIRIM group in which techniques for vapor growth of diamond on non-diamond substrates at rates of several microns per hour were described [14-16]. The current world wide interest in the new diamond technology can be directly traced to the NIRIM effort.

The great breakthrough in low-pressure diamond synthesis research came with the discovery that diamond growth is also possible on non-diamond

substrates [14]. The discovery of the metastable growth of diamond films using atomic hydrogen and carbon containing gases or vapors at pressures below atmospheric and not too high temperatures (600 to 1100 °C) has permitted diamond growth on non-diamond substrates like Si, Mo, Ta, etc., making it possible to obtain large diamond surfaces. Since then, a large number of potential applications were proposed, some of which are applied by now.

Currently, diamond synthesis from the gas phase under low pressure is routinely achieved by several different methods: hot filament, radio frequency plasma, glow discharge plasma, microwave plasma, arc discharge, electron assisted deposition, atomic vapor, and combustion flame[17].

The first diamond nucleation on substrates other than diamond by low pressure chemical vapor deposition (CVD) was produced in a hot filament reactor [15]. The hot filament method is one of the most common methods since it produces diamond easily and the equipment needed is less expensive than with most other methods, except for the flame method. The following sections describe the low pressure synthesis of diamond by hot-filament assisted chemical vapor deposition.

2.2 Low Pressure Synthesis

In the original reports of the metastable growth of diamond at low pressures, the growth rate of diamond was very small and diamond substrates were required, making the process of scientific interest only. Most methods stemmed from the work of Eversole who alternately exposed diamond substrates to a hydrocarbon gas and then hydrogen at temperatures of 950 to 1150 °C and low pressures of 0.15 torr. Under these conditions, the

hydrocarbon was pyrolysized to form diamond and graphite and then hydrogen was used to etch the graphite away. This cycle was repeated over and over again until the diamond deposit grew to the desired thickness.

$$CH_4 \xrightarrow{\text{Heat}} \text{Deposit (Diamond \& Graphite)} + 2\,H_2$$

$$H_2 + \text{Deposit} \xrightarrow{\text{Heat}} \text{Diamond} + CH_4$$

In the late 70's, an important invention changed this cyclic CVD (Chemical Vapor Deposition) process to a continuous one., increased the diamond growth rate by orders of magnitude, eliminated the need for diamond substrates and made the process technologically significant [21]. This new process is shown in reaction (1).

$$CH_4 \xrightarrow{\text{Heat \& Atomic Hydrogen}} \text{Diamond} + 2\,H_2 \qquad (1)$$

The key idea was the addition of atomic hydrogen to the reaction.

2.3 Hot Filament CVD Diamond Deposition Process

Langmuir first reported the dissociation of molecluar hydrogen on a hot tungsten filament in the early 1900's [18-20]. This was also the initial method that was used extensively to make atomic hydrogen in CVD diamond growth.

Typically, a hot filament is heated to a temperature range of 1950-2300 °C in the presence of molecular hydrogen and 1-2 % hydrocarbon. The molecular hydrogen adsorbs on the surface of the metal filament and dissociates into two atomic hydrogens that subsequently pass back into the surrounding gas.

H_2 ------> 2 H : H = +104 kcal/mole

In addition, many other reactions take place on the filament involving the hydrocarbon.

2.4 The Hot Filament Equipment

A schematic diagram of the hot-filament equipment for diamond deposition is shown later. A mixture of 1-2 % methane in hydrogen flows in through the gas inlet. The hot filament acts as a source for gas activation and thermal radiation. The total hot-filament surface determines the catalytic surface area actively involved in the formation of atomic hydrogen. Hence, the filament material and its properties are very important in the process. The filament is usually operated at temperatures of 1900 - 2200 °C. An increase in the filament temperature results in an increase in the substrate temperature because of higher heat radiation and higher atomic hydrogen recombination. However, increase in the filament temperature also results in contamination of the diamond film with filament elements.

Several types of filament designs have been used, including multiple filaments. Since the substrate temperature plays an important role in the quality

of diamond deposited on the substrate, there are also arrangements to heat or cool the substrate, other than through the radiant heating by the filament. The following sections describe the various filament and substrate materials that have been succesfully used in the hot-filament CVD process.

2.4.1 Filament material

There are some constraints on the electrically conductive refractory materials that can be used for atomic-hydrogen filaments. First, the melting point of the material must be higher than the operating temperature of the filament. Secondly, the binary eutectic temperature of carbon and the filament material must exceed the filament operating temperature to prevent the melting and breakage of the filament. Table 2.1 compares the relevant parameters for various filament materials.

The second requirement makes molybdenum filaments marginal since a hot spot on a molybdenum filament may take it above the Mo-C eutectic temperature of 2200 °C and cause the filament to melt and fail before the filament is fully carburized.

While a carbon filament satisfies the melting-point and eutectic-point requirements, it does not produce CVD diamond because atomic hydrogen that forms on a carbon filament reacts with the carbon and releases a hydrocarbon species into the gas rather than atomic hydrogen. Without atomic hydrogen at the substrate, graphite is deposited instead of diamond. The failure of carbon filaments to produce diamond suggests that the atomic hydrogen does not form in the hot gas surrounding the filament but actually forms on the filament surface [22].

Table 2.1: Parameters for various filament materials

Material	Melting Point	Evaporation Rate	Carbon Eutectic Point
	°C	grams/cm^2-sec	°C
Tungsten	3387	10^{-9}	2475
Carbon	3727	6×10^{-8}	3727
Rhenium	3180	7×10^{-5}	2486
Tantalum	2996	10^{-8}	2800
Molybdenum	2610	4×10^{-7}	2200
Niobium	2468	8×10^{-9}	2335

Of the remaining electrically conductive refractory materials, tungsten, tantalum and rhenium have been used to produce CVD diamond. Both tantalum and tungsten react with the hydrocarbon in the gas to form carbides. Thus, the tantalum and tungsten filaments quoted in the literature are really tantalum carbide and tungsten carbide filaments. Filament carburization can have a catalytic effect on the diamond nucleation rate by increasing the electron emission from the filament because of the lower work function of the carbide [23]. Electron bombardment of the substrate surface is also reported to increase the diamond nucleation rate [24].

2.4.2 Carburization

Carburization is a two stage process with M_2C forming first followed by MC where M is one of the refractory metals. Under typical hot-filament CVD diamond growth, M_2C forms in all cases. However, MC does not always form because the activity coeffecient of carbon is too small under some conditions of diamond growth. Since the carbides of tantalum and tungsten have a molar volume that is 40-70 % larger than the molar volume of the metal from which they form, the filaments swell, crack, bend, distort and embrittle as inward radial carburization proceeds. Carburization and cracking increase the electrical resistance of the filament; therefore, the current and voltage must be monitored and changed to maintain a constant filament temperature. Although cracking embrittles the filament, it produces an increased filament surface area which may increase the production of chemically active species required for diamond growth.

Rhenium is attractive because it does not form a carbide [25,26]. However, rhenium dissolves large amounts of carbon that causes rhenium to swell. In addition, the dissolved carbon may react with dissolved oxygen to form embrittling voids on grain boundaries. Thus, the annealed carbon-saturated rhenium wire is partially embrittled though much less so than either tungsten or tantalum. Rhenium, unfortunately is two orders of magnitude more expensive than tantalum or tungsten. Hence, tantalum and tungsten are the two most commonly used filament materials.

2.5 Substrate Materials

The heteroepitaxy of diamond via chemical vapor deposition (CVD) is a process of considerable technological importance. Many applications of diamond, especially in the area of microelectronics, await the growth of single crystal diamond on economically viable substrates. However, the heteroepitaxial growth of diamond films has not been successful despite several years of research using a wide variety of substrates. There is a general lack of understanding of the nucleation mechanisms of diamond under scientific conditions, which in turn hinders the development of techniques of surface preparation and interface engineering necessary for heteroepitaxial growth. Single crystal diamond films have only been grown homoepitaxially on diamond substrates.

Cubic boron nitride (cBN) has been considered an ideal substrate for diamond heteroepitaxy because of its close lattice match with diamond [1.3 % as defined by $(a_S-a_o)/a_S$, where a_S and a_o are lattice constants of the substrate and the diamond, respectively]. Diamond has been epitaxially grown on cubic

boron nitride crystals [27]. Unfortunately, cBN substrates of sufficient size to make the diamond growth practical are unavailable at the present time. Due to the extreme difficulty in obtaining single crystals of either diamond or cBN, other substrate materials were considered. Substrate materials studied include Si, Ni, Cu and refractory metals like W, Mo and Ta [28-34].

Sato *et al.* [35] reported the local epitaxial growth of diamond on Ni. Nickel has a close lattice match with diamond although its catalytic properties on the decomposition of hydrocarbons may make it difficult to inhibit the formation of graphite during diamond nucleation and growth.

Most of the experimental data on the nucleation of diamond on foreign substrates is available for single crystal silicon, as it is both inexpensive and easily available. However, recent studies by Stoner, Ma, Wolter and Glass [36] on the nucleation of diamond on silicon indicated the formation of silicon carbide on the silicon surface before the diamond particles could be detected.

The idea to use cubic silicon carbide (β-SiC) as a substrate for diamond heteroepitaxial growth originated from the observation that a silicon carbide interfacial layer exists between the diamond film and silicon substrate, and any observed local epitaxy of diamond on Si (34% lattice parameter mismatch between diamond and Si) is most likely a result of limited diamond epitaxial growth on the interfacial silicon carbide layer (18% lattice parameter mismatch). However, it was found that the initial nucleation of diamond on a clean, undamaged β-SiC surface was not possible [37].

Hence, it is clear that the lattice parameter mismatch and the interface chemistry are not the only restricting factors for diamond growth on silicon.

2.6 Nucleation of Diamond

Before attacking the specific problem of diamond nucleation, the basic steps involved in the nucleation of three-dimensional clusters should be considered. General cluster-nucleation phenomena may be simplified and explained as a series of the following steps [38].

(i) Atoms impinge upon the substrate from the vapor phase and become adsorbed onto the surface.

(ii) At standard CVD conditions, the adsorbed atoms, if they are not free to react with the substrate, may either reevaporate or diffuse over the surface.

(iii) If the combination of adsorbed atoms is high enough, they may combine and form clusters.

(iv) Through statistical fluctuations in local adsorbed atom concentration, these clusters grow or decay.

(v) Because of free energy considerations, there will be a critical size above which the probability of growth will be greater than decay.

(vi) These stable clusters are free to grow either from the continued migration of single adsorbed atoms or from the direct impingement of atoms from the vapor phase.

2.7 Methods of Surface Treatment for Nucleation Enhancement

The nucleation density of diamond on mirror-polished surfaces, using the hot filament process is low. The nucleation density on untreated silicon was found to be about 10^4 cm^{-2}. At such low densities it is difficult to obtain continuous films in a reasonable time due to the slow rate of deposition (usually

1μm per hour) in the HF method. Several hypotheses for heterogeneous diamond nucleation onto foreign substrates have also been made, based on experimental observations on treated substrates.

2.7.1 Scratching the substrate

It is well known that the diamond nucleation density may be increased by several orders of magnitude by simply scratching, abrading or blasting the substrate surface with a fine diamond powder or paste, prior to placing it into the growth chamber. Another method is scratching the substrate surface in an ultrasonic vibrator using diamond paste diluted in methanol or acetone. The ultrasonically damaged surface has uniformly distributed defects and the results obtained on such surfaces are more reproducible. By this technique nucleation densities of about 10^9 cm^{-2} are obtained on silicon substrates. Although various cleaning methods are used, the complete removal of carbon deposited in polishing cannot be assumed. The correlation in many experiments between the scratches left by polishing with diamond powder, and the subsequent nucleation and growth of diamond crystal is unmistakable and two major schools of thought have been advanced to explain the efficacy of polishing with diamond.

The first argues that polishing with diamond leaves diamond particles, or an ill defined carbonaceous residue. Bachmann *et al.* [39] postulated that residual diamond particles left on the surface from the scratching medium acted as diamond nucleation sites. This is based on the fact that diamond will tend to nucleate preferentially on the diamond seeds, thus resulting in discrete homoepitaxy of diamond. Iijima, Aikawa, and Baba provided direct observation

of high resolution transmission electron microscopy (HRTEM) of diamond nucleation on "diamond seeds" left from the scratching process [40,41]. However, abrading the substrate with nondiamond abrasives such as cubic boron nitride (cBN) [42], silicon carbide [43], and stainless steel [44] has also yielded high nucleation densities.

The second of these maintains that the damage done by polishing enhances nucleation by creating high surface free energy damage sites. However, despite extensive TEM work, there is no conclusive proof that the high surface-defect density is responsible for enhanced nucleation density. A variation on this idea is the suggestion that polishing removes surface contaminants or strongly adherent films which could inhibit nucleation. Diamond nucleation is also favored on prominent features of the substrate surface, that is, surface morphologies that protrude with sharp edges or points, as opposed to valleys or flats. Such features are created by scratching before growth. Dennig and Stevenson [45,46] observed selected growth on the prominent features of chemically etched surfaces. It has been speculated that the total free energy of a diamond embryo is lowered by securing some minimized contact area with the substrate, thereby favoring nucleation at these morphological features. Yugo *et al.* [47], in their studies on diamond growth by plasma CVD, investigated the correlation between the shape of scratches and generation of diamond nuclei. Using STM images of a mirror polished silicon surface and ultrasonically treated silicon surface, they concluded that scratches with depth of about 10 nm act as effective centers for the generation of nuclei and that randomly distributed small scratches with depth below 5 nm suppress the generation of nuclei.

2.7.2 Covering the surface with carbon phases

Besides the widely used method of surface damaging discussed above, that increase the nucleation density, some other methods to enhance the nucleation density were proposed. Covering the surface by carbon phases other than diamond: diamond-like carbon (DLC), amorphous carbon, bucky balls, or carbon containing substances like oil, does enhance the diamond nucleation density [48-51].

Morrish and Pehrsson [51], compared from the nucleation point of view, substrates scratched by diamond grit and then coated with either pump oil or evaporated carbon film 10 to 20 nm thick. Both treatments enhanced the nucleation density as compared to the noncovered samples. Continuous films were obtained on diamond scratched and oil coated molybdenum substrates, while the diamond crystals on non-oil-treated substrates were less numerous. Similar results were also obtained on silicon substrates.

Ravi *et al.* [49,50] found that diamond-like films formed on Mo substrates in the combustion flame method enhanced the diamond nucleation density by an order of magnitude as compared to the deposition on abraded Mo and molybdenum carbide.

Another recent technique for nucleation enhancement, used by Stoner and Glass [52-54] , is to simply bias the substrate negatively while immersed in a methane hydrogen plasma.

2.7.3 Interface chemistry

Interface chemistry is also important in the diamond nucleation process. Williams and Glass [55] observed an interfacial β-SiC layer between the silicon substrate and the diamond film grown at 0.3 % methane by cross-sectional TEM and again by x-ray photoelectron spectroscopy (XPS). Since then, carbide formation on various substrates has been observed prior to diamond nucleation and growth by many other researchers. Joffreau, Haubner, and Lux [56] performed a systematic study of diamond growth on refractory metals and observed that diamond nucleation occurred only after the formation of a thin carbide layer. However, there are contradictory reports on the nucleation of diamond on untreated bulk SiC substrates. Zhu *et al* [37] have reported that their attempts to grow diamond on clean, undamaged bulk SiC substrates did not yield high nucleation densities. Others have reported favorable growth on SiC [57,58] with nucleation densities only a few times greater than on untreated silicon. Stoner, Ma, Wolter, and Glass [36], in their study of the nucleation of diamond on silicon by bias-enhanced microwave plasma chemical vapor deposition, have observed an amorphous silicon carbide layer at the diamond-silicon interface.

Hence, the importance of the carbide surface condition and the exact role it plays in the promotion of diamond nucleation are unclear.

2.8 Introduction to Ion Implantation

Investigation of ion bombardment as a method for alteration of the electrical properties of semiconductors began in the late 1950's. In the 1970's

ion implantation was explored as a method for surface modification of metals [59]. The technique is now routinely used as a surface modification tool.

In the ion implantation process, ions are accelerated to energies ranging from tens to hundreds of kiloelectron volts, and are directed towards the surface of the target material. As the ions enter the target, they collide with electrons and nuclei of the target, thus losing their energy and coming to rest. The implanted ions have an approximately Gaussian distribution which peaks a few hundred nanometers below the target surface.

The collisions between the impinging atoms and the target atoms displace some of the target atoms from their normal lattice sites. Large numbers of point defects are produced over a range of depths from a few hundreds to a few thousands of atomic distances from the target surface [59]. At high ion doses, extensive displacement damage occurs, and a sub-surface amorphous zone may be produced in the target material. This layer thickens with still increasing dose, eventually becoming a surface amorphous layer [60].

Ion implantation has several advantageous features which make it useful, both as a research tool and as a practical method for surface property control. The technique allows independent control of the number of ions implanted and their depth. A number of ion/target combinations exists. Since the process is non-equilibrium in nature, structures and compositions may be produced which are non-attainable by conventional means.

CHAPTER 3

MOTIVATION FOR THIS WORK

The understanding of the nucleation phenomena of heteroepitaxial diamond is of prime interest if the scientific community is to take full advantage of this material's extreme and superior properties. As is discussed in the preceding sections, interface chemistry and surface defects seem to play very important roles in the nucleation of CVD diamond on various substrates.

Many nucleation mechanisms have been proposed based on the belief that the formation of a SiC layer precedes the nucleation of CVD diamond on Si. It is also widely believed that some of the surface defects created by abrasion with diamond powder prior to diamond growth act as nucleation sites, accounting for the increase in the nucleation density compared to nucleation on pristine substrate surfaces.

Both Si or C faced single crystal 6H silicon carbide substrates were used in this study. The properties of the substrate are listed on the material data sheet in the appendix. The motivation to use 6H silicon carbide originated from the above mentioned observation of the interfacial SiC layer and the fact that the lattice mismatch between diamond and the 6H silicon carbide substrate is only 16 % compared to the 18 % mismatch with β SiC.

This work was primarily aimed at studying the effect of surface defects on the nucleation of diamond on 6H SiC. Defects on the atomic scale, like vacancies and interstitials can be created on the substrate surface by the process of ion-implantation. Carbon and silicon ions at different fluences were implanted on both the as received and the abraded silicon carbide substrates,

with a view to do a comparative study of the nucleation effects in the various cases.

Will diamond nucleate on undamaged 6H silicon carbide ? Will the surface defects created by ion-implantation enhance the nucleation of diamond on the silicon carbide ? Does the type of external face (C or Si) influence the nucleation density ? What will be the effect of ion-implantation on SiC samples already abraded using diamond paste ?

All the above questions were desired to be answered through this investigation using the hot-filament CVD process.

CHAPTER 4

EXPERIMENTAL PROCEDURE

4.1 Substrate Treatments

The substrates for this study were single crystal (0001) 6H silicon carbide. The 1 inch diameter 6H SiC wafers were obtained from CREE Research Inc. There were two types of substrates- one with the polished side being the silicon face and the other with the carbon face on the polished side. The wafers were cut into small samples (7 mm x 12 mm), using a diamond scribe.

4.1.1 Polishing

One wafer of each type of substrate was polished for 30 minutes in an ultrasonic vibrator using 20 μm diamond powder suspended in ethanol. After polishing, the wafers were cleaned with alcohol and acetone to remove any residual diamond particles. Each wafer was then cut into smaller samples for implantation.

After the polishing treatment, there were four different types of substrates- as-received sample with Si face, as-received sample with C face, diamond polished sample with Si face, diamond polished sample with C face.

4.1.2 Ion Implantation

One half of each sample was masked before implantation to perform a comparitive study of the nucleation density between the implanted and non-implanted areas. Both carbon and silicon ions were used for implantation. The

samples were implanted at 77 K in order to prevent diffusion of vacancies and interstitial atoms during implantation. Implantation was done at a tilt of 6° to prevent any chanelling. Five different implantations were done on each of the four above mentioned types of substrates. Si^{29} ions at 150 keV and C^{12} ions at 55 keV were used for implantation. The first implantation was done with a fluence of 2×10^{14} Si^+ cm^{-2} in order to introduce defects in the substrate surface without destroying the crystallinity. A second implantation with a fluence of 4×10^{14} Si^+ cm^{-2} was done in order to damage the substrate surface and retain only a partly crystalline surface layer. The third implant involved a fluence of 2×10^{15} Si^+ cm^{-2} to create a completely amorphous layer at the surface. The fourth set of samples were implanted with a fluence of 4×10^{14} C^+ cm^{-2} to damage the surface without destroying the crystallinity. The final implant was a dual implantation of silicon and carbon (2×10^{15} Si^+ cm^{-2} at 150 keV and 4×10^{14} C^+ cm^{-2} at 55 keV) .

RBS/chanelling was used to measure the depth and degree of damage in each crystal. 2 MeV He^+ ions were used. Backscattered ions were detected at 160° to the incoming beam and a gain of 150x was used.

4.2 Diamond Deposition

The diamond nucleation phenomena investigated in this work was performed by the hot filament assisted CVD technique. A schematic diagram of the experimental setup is shown in Figure 4.1 and the deposition chamber is shown in Figure 4.2 . The gas used in this study contained 0.5 % methane in hydrogen and was supplied in pre-mixed high pressure cylinders. The gas mixture flowed through a pressure regulator and a mass flow controller and finally into the

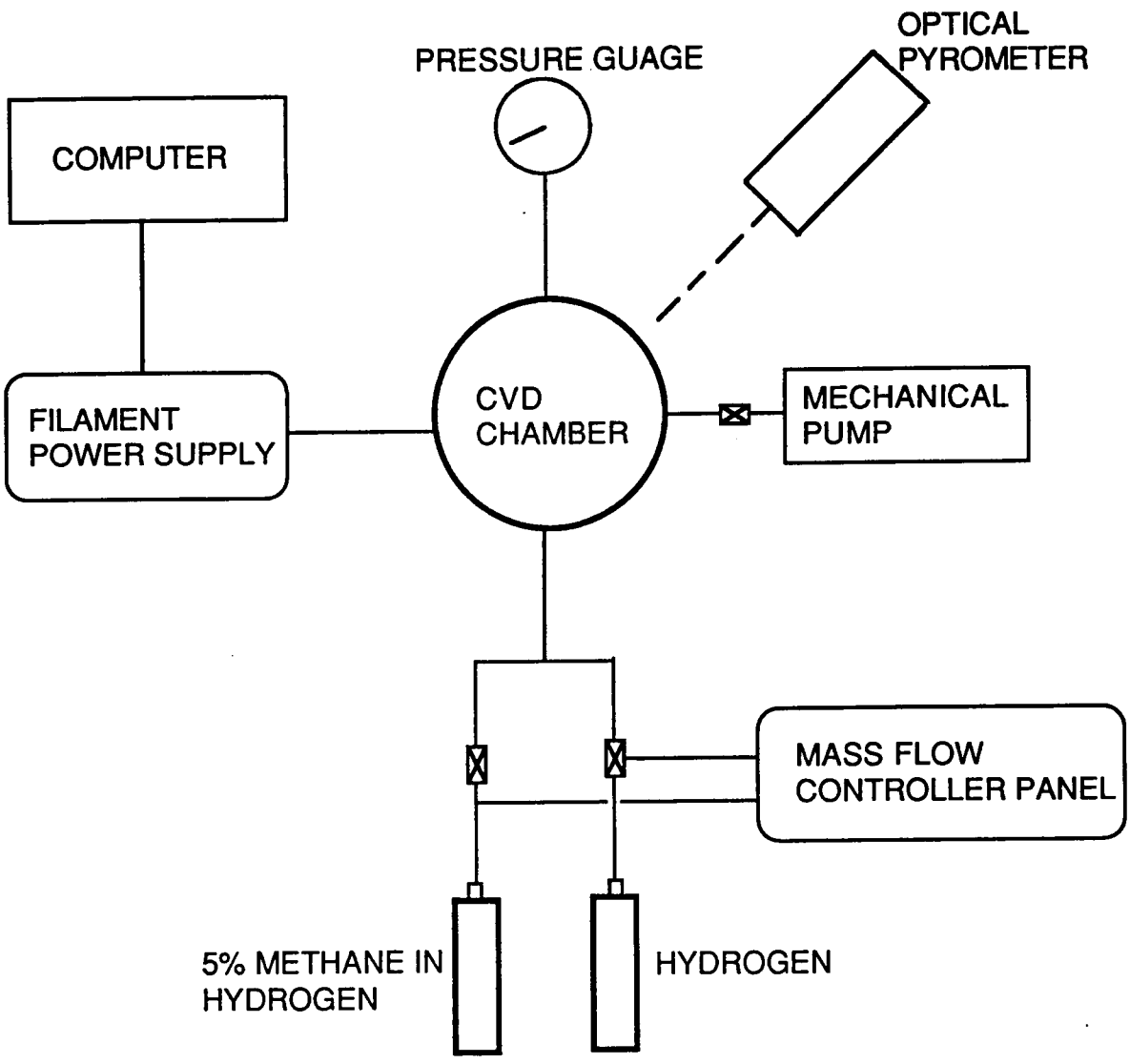


Figure 4.1 Schematic diagram of the experimental setup used for diamond deposition in this study

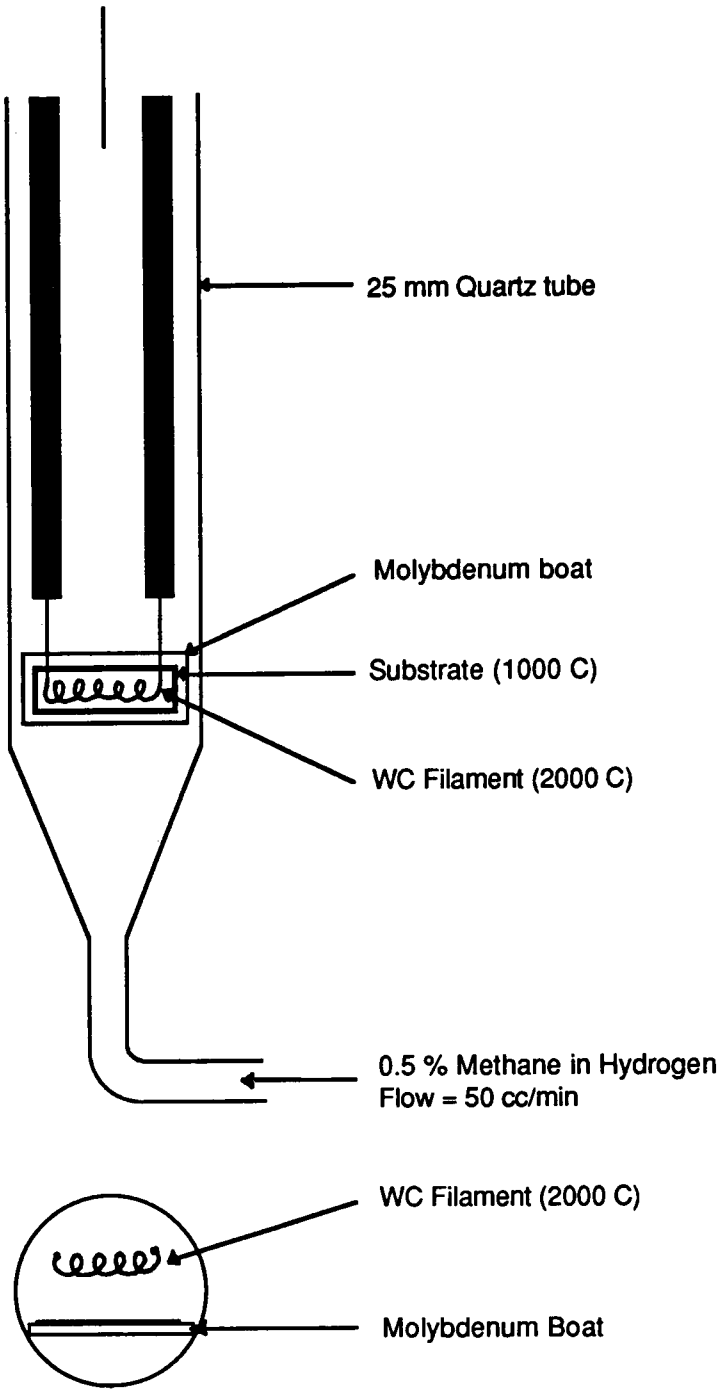


Figure 4.2 Design of a CVD chamber for diamond deposition can be very simple.

deposition chamber. The depostion chamber is a quartz tube of diameter 25 mm with a tapered end through which the gas flowed in. After being activated at the hot filament, the products reached the substrate through a combnation of flow and diffusion processes. The gas was then pumped out through the larger end of the quartz tube with a direct drive mechanical pump. The flow rate for the gas mixture during these investigations was 50 std. $cm^3\ min^{-1}$, and the chamber operating pressure was 5.3 kPa (40 Torr).

The filament was fabricated by wrapping several turns of tunsten wire (diameter 0.5 mm) around a mandril (diameter 3 mm). The tungsten wire was first cleaned, using a SiC sheet (400 mesh), to remove surface coatings, if any. It was then cleaned with alcohol, before being wrapped into a filament. The coil was again rinsed with alcohol to remove any dirt, fingerprints. etc.

A stable current-controlled direct current power supply was used to heat the filament to the desired temperature. The substrate was heated by radiant heat from the filament to a temperature of 1000 °C. The substrate holder was fabricated from a small piece of molybdenum sheet and the substrate was placed below the filament in the molybdenum boat which acted as a radiant heat baffle (reflector).The temperature of the substrate was measured optically by looking at the back of the substrate through two small holes in the molybedenum boat (substrate holder). The temperature measurements were made using a disappearing filament optical pyrometer. The same pyrometer was used to measure the filament temperature through the quartz tube.

A new filament was first annealed in vacuum for 1 minute to relieve any stresses generated due to coiling after which it was carburized for a period of atleast 2 hours before the study was conducted. Carburization was done at the

same conditions of diamond nucleation as described above. During this process, the filament temperature had to be adjusted to maintain a constant value. This was achieved by using a computer connected to the power supply. The computer program sets the filament power to a constant value and adjusts the filament current and voltage to maintain this value. This maintains a fixed filament temperature. After carburization of the filament, the temperature remains almost constant.

Diamond deposition was done for 30 minutes so that only isolated particles were formed instead of a continuous film. The conditions for the CVD process are given below:

Hydrogen gas flow rate	45 sccm
5% methane in hydrogen flow rate	5 sccm
Chamber pressure	40 torr
Filament temperature	2100 °C
Substrate temperature	1000 °C
Filament material	Tungsten (W)
Substrate material	SiC (C or Si face)
Substrate to filament distance	8 mm

4.3 Scanning Electron Microscopy

The nucleation density of CVD diamond on the silicon carbide substrates was determined using a Hitachi S 800 high resolution scanning electron microscope (SEM) equipped with a field emission gun. The SEM was operated at 20 kV. High magnification SEM micrographs of the various regions under

study were taken and analysed to calculate the nucleation density. This was done by counting the total particles in a micrograph and dividing it by the total area on the micrograph. Comparision of data was done using micrographs of areas across the region separating the implanted and non-implanted region of each sample.

CHAPTER 5

RESULTS AND DISCUSSION

SEM studies on the as-received (polished after crystal growth but not before diamond deposition) samples after chemical vapor deposition (CVD) showed no nucleation either on the non-implanted or implanted samples. This was true for both the silicon and the carbon faced samples. Nucleation was observed in only certain areas where there was some residual dirt or other matter after cleaning in alcohol. This is in agreement with the reports in literature that nucleation is enhanced by covering the substrate surface with carbon phases [48-51].

Abrasion of the silicon carbide substrate in an ultrasonic vibrator with 20 μm diamond powder dispersed in ethanol greatly enhanced the nucleation of diamond on both the Si and C faced samples. Figure 5.1 shows a low magnification image of diamond on an abraded sample. Both the implanted and non-implanted regions on the sample show diamond nucleation. The implanted region looks darker when compared to the clear non-implanted region. Figure 5.2 shows the same region at a higher magnification. This difference in color between the implanted and non-implanted regions is true for all samples in this study.

Figure 5.3 shows the diamond nucleation on the unimplanted surface of a silicon faced sample. The nucleation density was calculated to be 6.00×10^9 cm^{-2}. Figure 5.4 shows diamond nucleation on the implanted region (2×10^{14} Si^+ / cm^2, 150 keV) of the same sample. The nucleation density was calculated

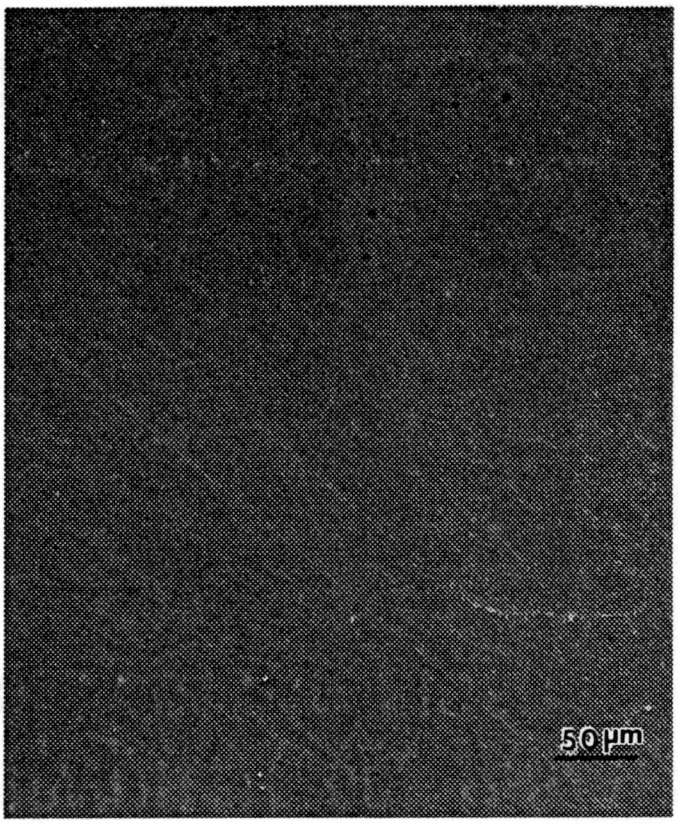


Figure 5.1. Low magnification scanning electron micrograph showing diamond nucleation on a sample abraded with diamond powder in the ultrasonic vibrator. The implanted region is darker compared to the non implanted region.

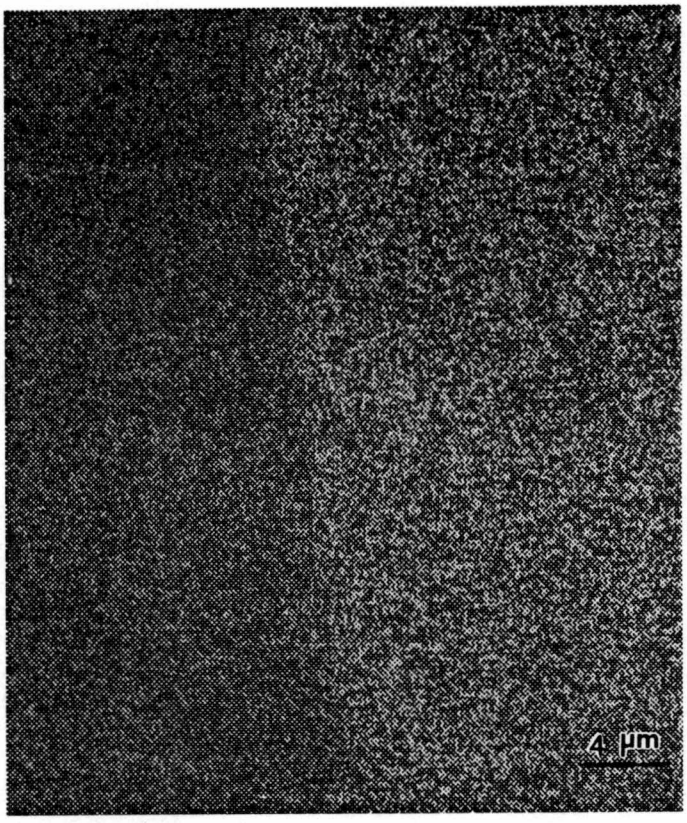


Figure 5.2. Scanning electron micrograph showing diamond nucleation on a sample abraded with diamond powder in the ultrasonic vibrator. Higher magnification reveals the presence of nucleated diamond and contrasts the implanted and non implanted regions.

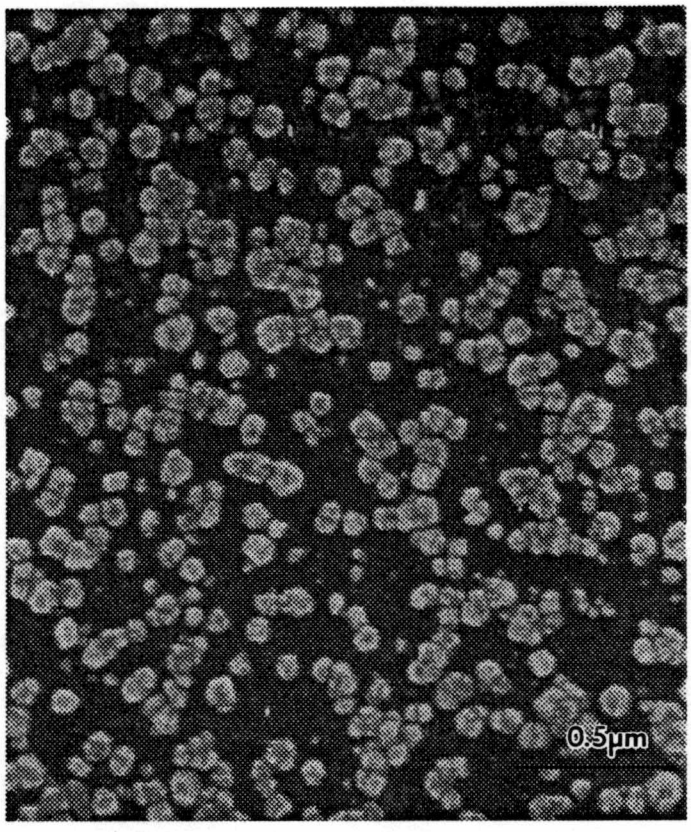


Figure 5.3. Scanning electron micrograph showing high diamond nucleation density on the non implanted surface of a Si faced sample. Nucleation density = 6×10^9 cm^{-2}

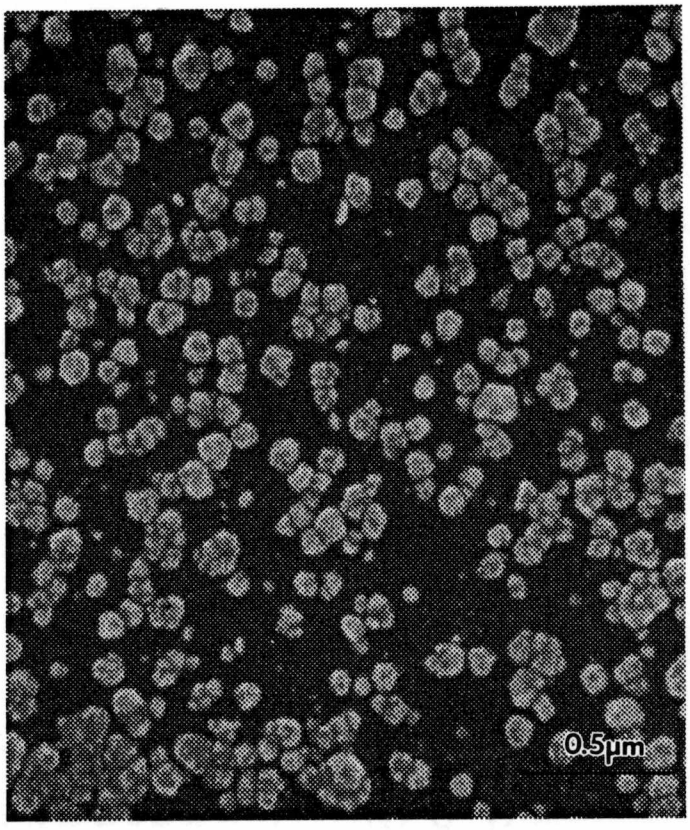


Figure 5.4. Scanning electron micrograph showing diamond nucleation on the implanted surface (2 x 10^{14} Si^{+} cm^{-2}, 150 keV) of a Si faced sample. Nucleation density = 5.95 x 10^{9} cm^{-2}

to be 5.95 x 10^9 cm^{-2} which is very close to the above value of nucleation density.

Figure 5.5 shows the diamond nucleation on the unimplanted region of C faced sample. The nucleation density was calculated to be 4 x 10^9 / cm^2 . Figure 5.6 shows the implanted region (2 x 10^{14} Si^+ / cm^2, 150 keV) of the same sample. The nucleation density is 3.8 x 10^9 / cm^2 which is slightly lower than the above value.

Both the silicon and carbon faced samples were subjected to similar pretreatment before diamond growth. On comparison of the nucleation densities, it is seen that the nucleation density is higher for the Si faced sample compared to the C faced sample. Also, the micrographs show that the particle size is slightly larger in case of the C faced sample. This implies that nucleation of diamond occurs more easily on Si faced samples whereas growth of diamond nuclei is faster on carbon faced samples.

Figure 5.7 shows the effect of increasing fluence of Si^+ ions (4 x 10^{14} Si^+ / $cm^{2)}$ on the nucleation of diamond on Si faced samples. The increase in the particle size in these micrographs suggests that the growth parameters may have been changed. The nucleation density is 3.34 x 10^9 / cm^2 compared to a nucleation density of 4 x 10^9 / cm^2 on the unimplanted region of the same sample (Figure 5.8).

The unimplanted regions on all the samples with the same external face (Si or C) should show similar nucleation densities if all the experimental parameters remain the same. However, the differences in the nucleation densities on the unimplanted sides suggest that the data be standardized before analysis. This was done by assuming that the nucleation densities on the

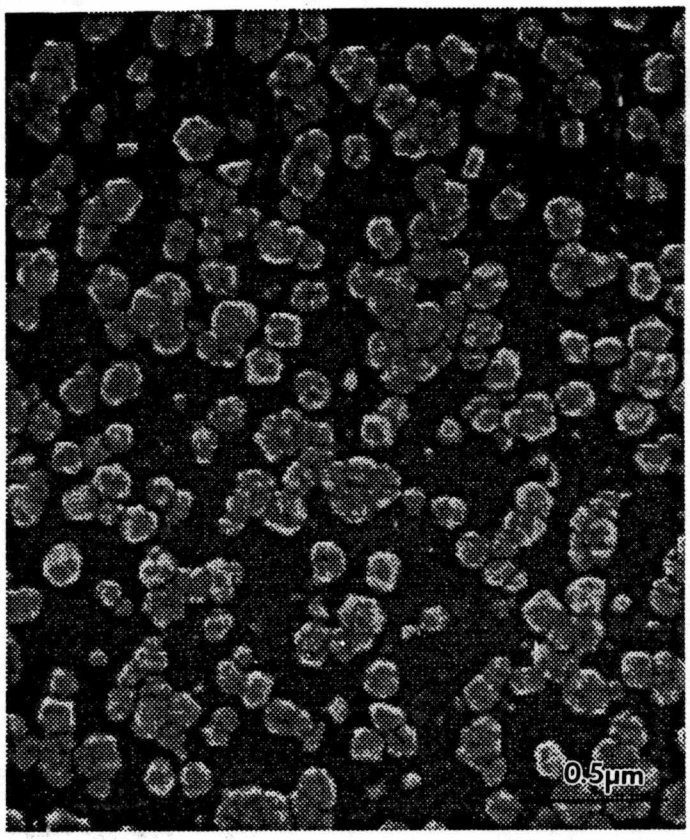


Figure 5.5. Scanning electron micrograph showing diamond nucleation on the non implanted region of a C faced sample. Nucleation density = 4.0 x 10^9 cm^{-2}

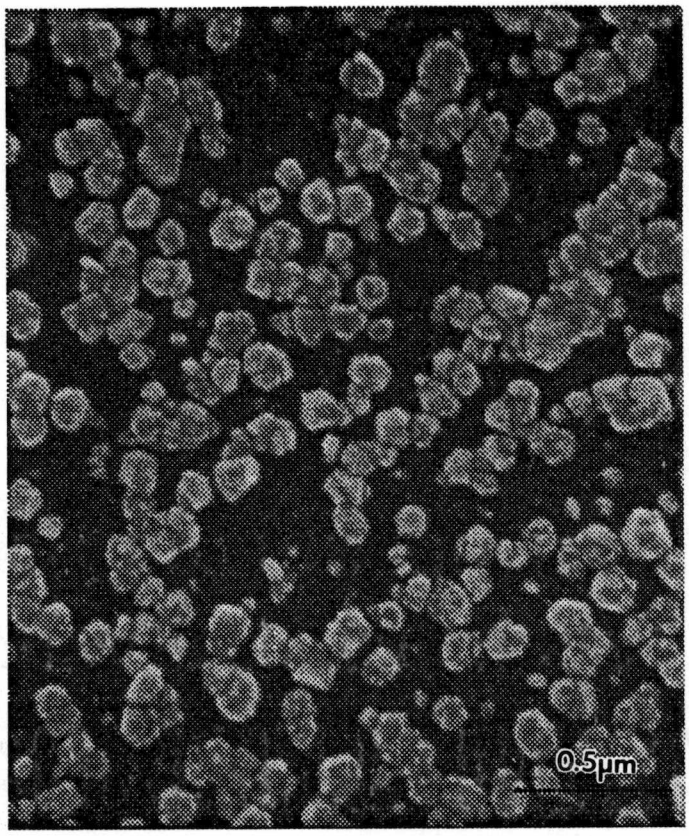


Figure 5.6. Scanning electron micrograph showing diamond nucleation on the implanted region (2 x 10^{14} Si^{+} cm^{-2}, 150 keV) of a C faced sample. Nucleation density = 3.8 x 10^{9} cm^{-2}

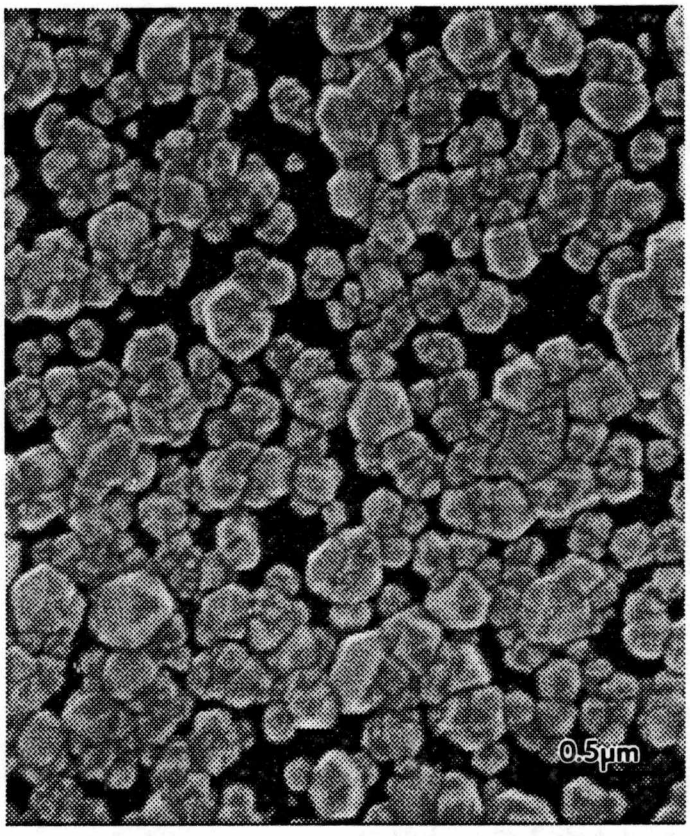


Figure 5.7. Scanning electron micrograph showing diamond nucleation on the implanted region (4 x 10^{14} Si^{+} cm^{-2} , 150 keV) of a Si faced sample. The diamond particle size has increased (compare to earlier micrographs). Nucleation density = 3.34 x 10^{9} cm^{-2}.

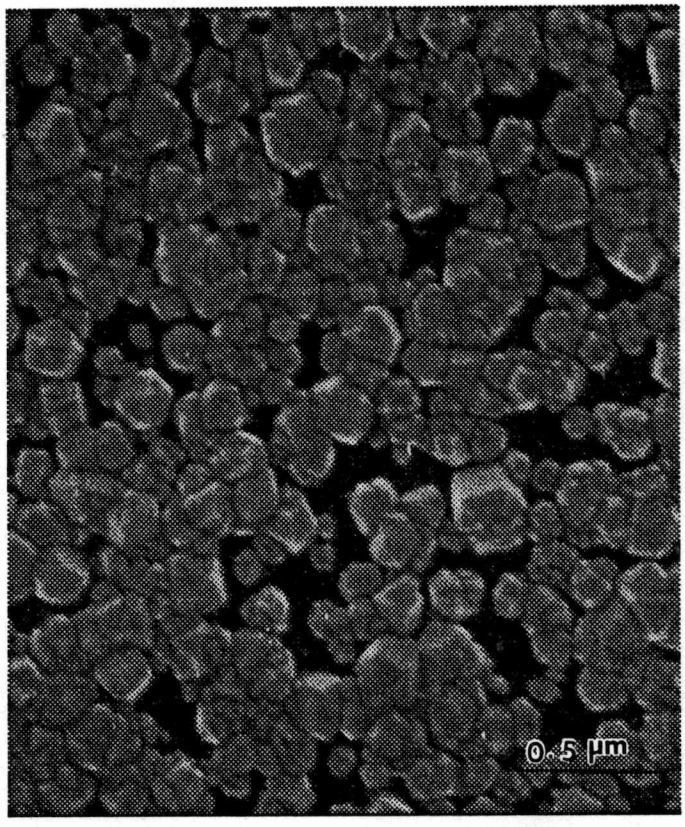


Figure 5.8. Scanning electron micrograph showing diamond nucleation on the non implanted region of the same Si faced sample as in figure 5.7. Nucleation density = 4.0×10^9 cm^{-2}

non-implanted regions of all the abraded samples were 6.00 x 10^9 cm^{-2} and 4.00 x 10^9 cm^{-2} for the Si faced and C faced samples respectively. The nucleation density for each of the implanted regions was then calculated by using the relation:

Calculated nucleation density on implanted region = [Observed nucleation density on implanted region / Observed nucleation density on non implanted region] x [Assumed value on non implanted region].

Carbon faced samples implanted with 4 x 10^{14} Si^+ / cm^2 at 150 keV showed similar effects as seen in the Si faced samples. Figures 5.9 and 5.10 illustrate these effects of decreasing nucleation density with increasing fluence of implanted ions.

Figure 5.11 shows the difference in diamond nucleation between the unimplanted and implanted (2 x 10^{15} Si^+ / cm^2, 150 keV) regions of a Si faced sample. There is no nucleation on the implanted region of the sample and there exists a demarcation between the two regions. Similar results are also seen on the carbon faced samples implanted with 2 x 10^{15} Si^+ / cm^2 at 150 keV (Figure 5.12).

Carbon implantation (4 x 10^{14} C^+ cm^{-2} , 55 keV) on the abraded samples before diamond growth did not produce any difference in nucleation between the unimplanted and implanted regions, on either of the two types of samples (Si and C face). Only one fluence of carbon implantation was performed. Hence, the effect of increasing dose of carbon implantation could not be studied.

Figure 5.13 shows the effect of the dual implantation (2 x 10^{15} Si^+ / cm^2, 150 keV followed by 4 x 10^{14} C/ cm^2 , 55 keV) on the Si faced sample. There

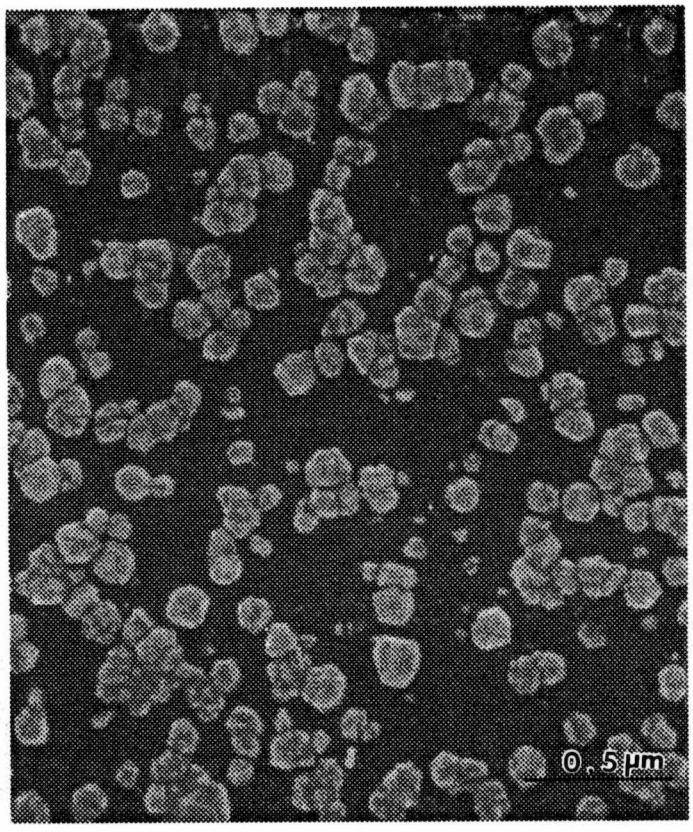


Figure 5.9. Scanning electron micrograph showing diamond nucleation on the non implanted region of a C faced sample . Nucleation density = 3.3 x 10^9 cm^{-2}

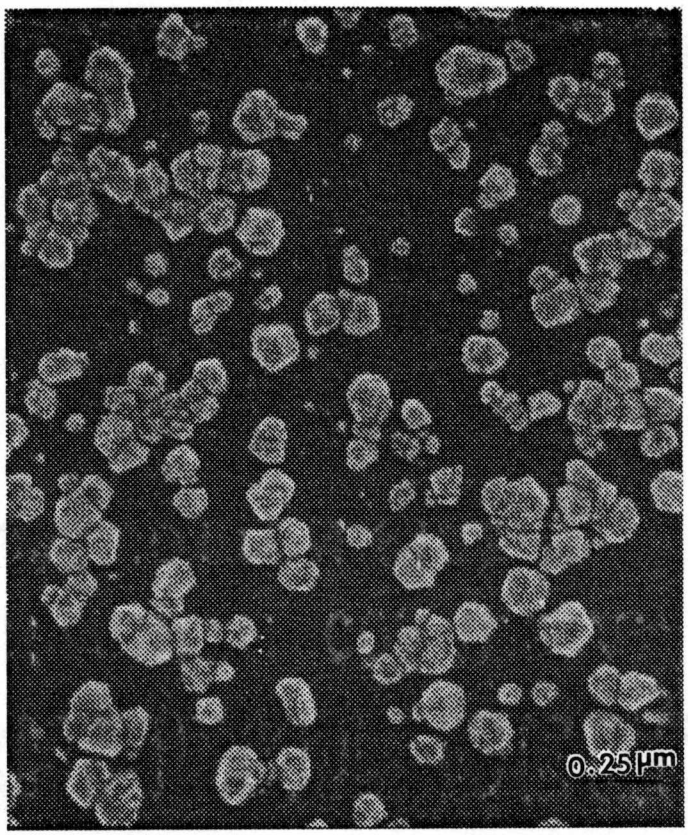


Figure 5.10. Scanning electron micrograph showing diamond nucleation on the implanted region (4 x 10^{14} Si^{+} cm^{-2}, 150 keV) of a C faced sample . There is a decrease in nucleation density (compare with Figure 5.9). Nucleation density = 2.43 x 10^{9} cm^{-2}

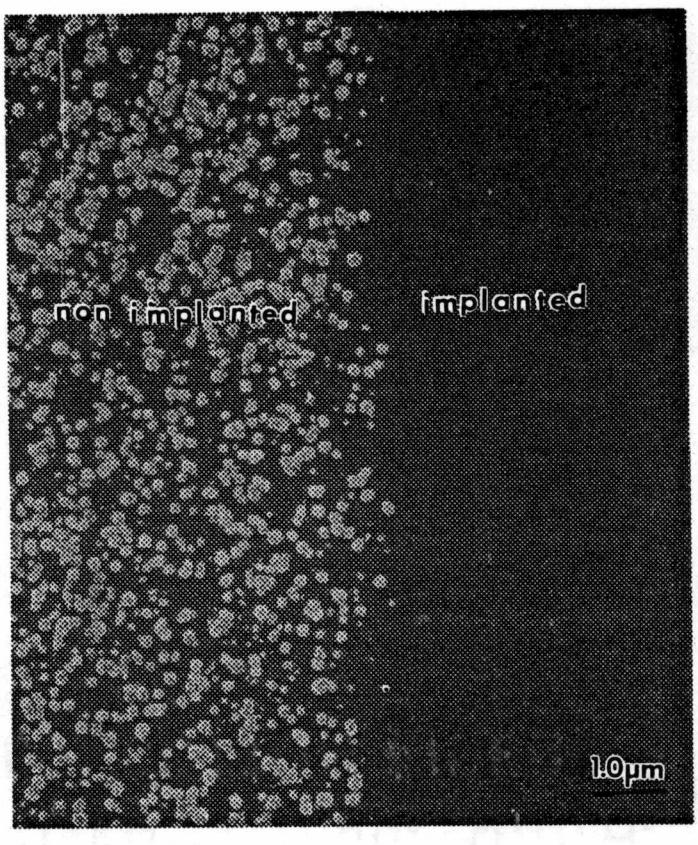


Figure 5.11. Difference in diamond nucleation between the non implanted and implanted region (2 x 10^{15} Si^{+} cm^{-2}, 150 keV) of a Si faced sample . No nucleation occurs on the implanted region.

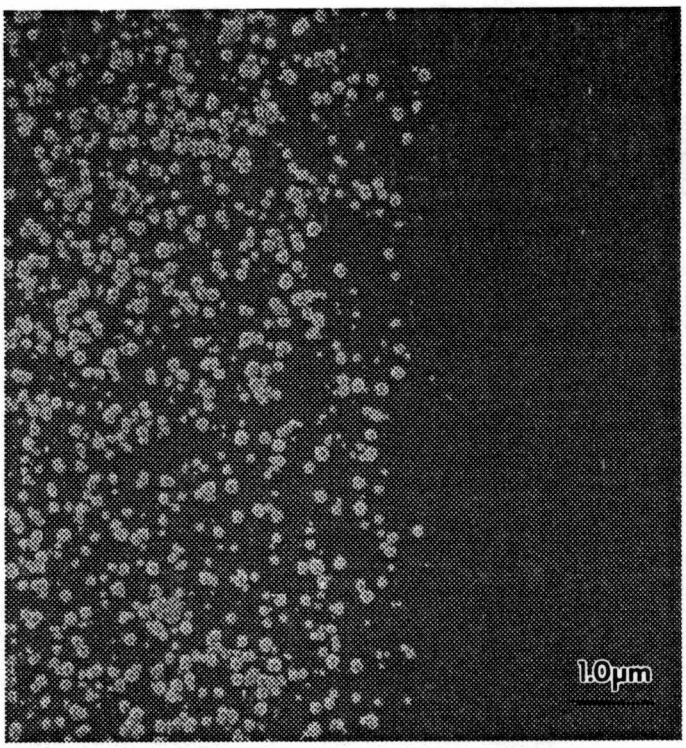


Figure 5.12. Difference in diamond nucleation between the non implanted and implanted regions (2 x 10^{15} Si^{+} cm^{-2}, 150 keV) of a C faced sample . No nucleation occurs on the implanted region as in the case of the Si faced sample..

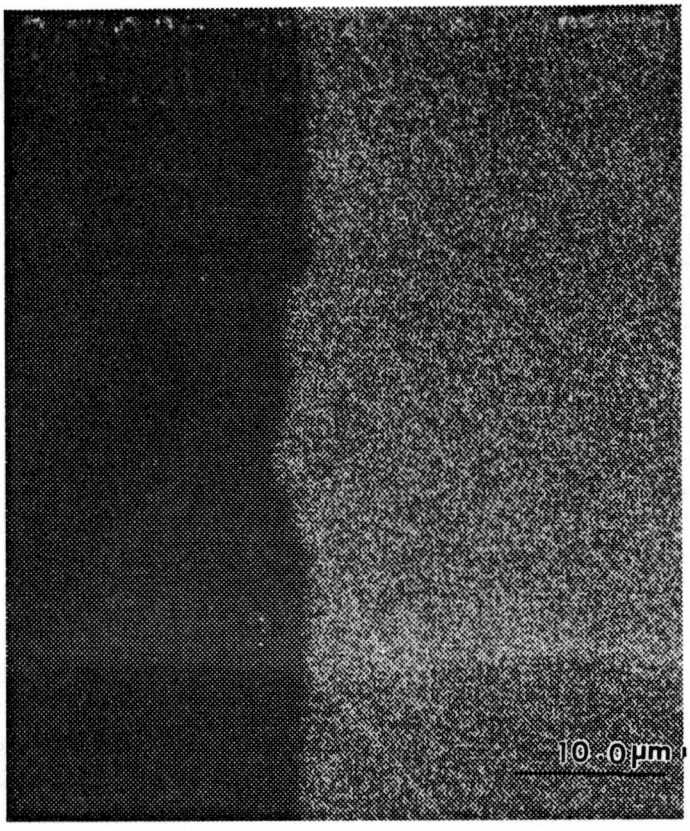


Figure 5.13. Effect of Si implantation (2 x 10^{15} Si^{+}/cm^{-2}, 150 keV) followed by C implantation (4x 10^{14} C^{+}/cm^{-2}, 55 keV) on a Si faced sample. No effect of added carbon implantation. Fine demarcation between implanted and non implanted regions.

seems to be no effect of the added carbon implantation. There is no nucleation on the implanted region. Figure 5.14 illustrates the same effect in the case of the dual implanted C faced sample. Similar effects are seen in both the silicon and the carbon faced samples.

The raw data of nucleation density values are shown in Table 5.1. The standardized values of the nucleation densities are shown in Table 5.2. Figure 5.15 is a graph of the nucleation density of diamond on Si faced SiC versus the fluence of implanted silicon ions. It is clear that the nucleation density decreases with increasing fluence of implanted ions. The same effect is seen for the C faced samples as illustrated in Figure 5.16. Figure 5.17 suggests that the nucleation density is lower in case of the C faced samples when compared to the Si faced samples under similar surface pretreatment conditions.

Literature reports that the nucleation density can be increased by covering the surface of the substrate with carbonaceous phases [48-51]. One may be inclined to assume that the carbon faced sample would show higher nucleation. However, the results show that this is not true. Also, carbon implantation on SiC would have a distribution of carbon on the surface. This again suggests an increase in nucleation density with carbon implantation, which is not seen in this study.

RBS/channeling studies on the implanted silicon carbide samples show the nature of damage to the substrate surface. If the surface of the substrate is crystalline, the back scattering yield would be low if the beam is in a channeling direction. The back scattering energy from a high atomic weight element would be higher compared to that from a low atomic weight element. When the surface is damaged and crystallinity is lost, channeling would produce peaks because

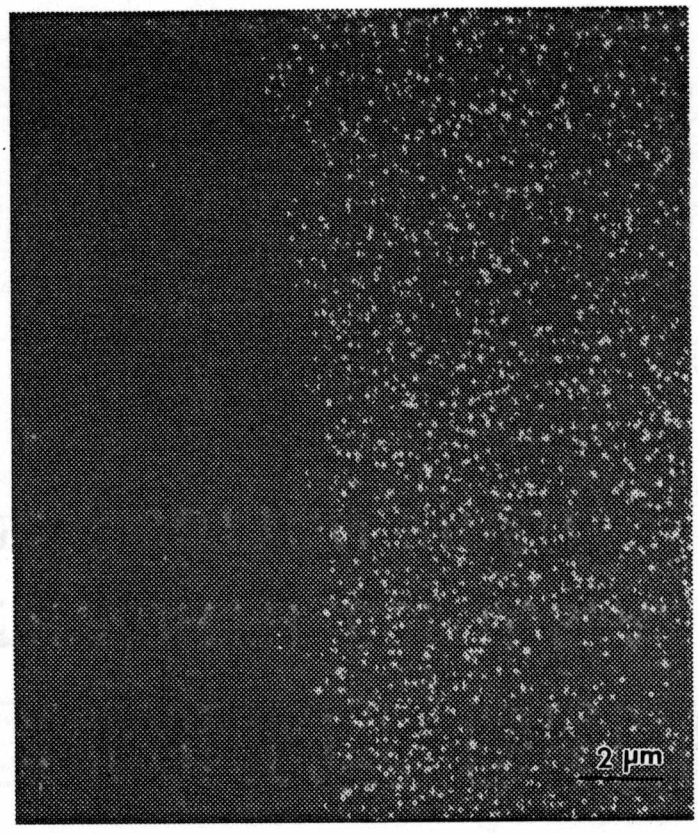


Figure 5.14. Effect of dual implantation (Si^+ followed by C^+) on a C faced sample. Similar effects as observed in figure 5.12.

Table 5.1. Nucleation density of diamond on 6H SiC (Raw Data)

Implantation Dose	Nucleation density (per sq. cm)			
	Si faced 6H SiC		C faced 6H SiC	
	Non implanted	Implanted	Non Implanted	Implanted
2E14 Si/sq. cm	6.00E+09	5.95E+09	4.00E+09	3.80E+09
4E14 Si/sq. cm	4.07E+09	3.34E+09	3.28E+09	2.43E+09
2E15 Si/sq. cm	2.71E+09	0	1.95E+09	0
4E14 C/sq.cm	1.19E+09	1.16E+09	2.00E+09	1.96E+09
2E15 Si/sq. cm & 4E14 C/sq.cm	3.12E+09	0	6.86E+08	0

Table 5.2. Nucleation density of diamond on 6H SiC (Standardized Data)

Implantation Dose	Nucleation density (per sq. cm)			
	Si faced 6H SiC		C faced 6H SiC	
	Non implanted	Implanted	Non Implanted	Implanted
2E14 Si/sq. cm	6.00E+09	5.95E+09	4.00E+09	3.80E+09
4E14 Si/sq. cm	6.00E+09	4.92E+09	4.00E+09	2.96E+09
2E15 Si/sq. cm	6.00E+09	0	4.00E+09	0
4E14 C/sq.cm	6.00E+09	5.84E+09	4.00E+09	3.92E+09
2E15 Si/sq. cm & 4E14 C/sq.cm	6.00E+09	0	4.00E+09	0

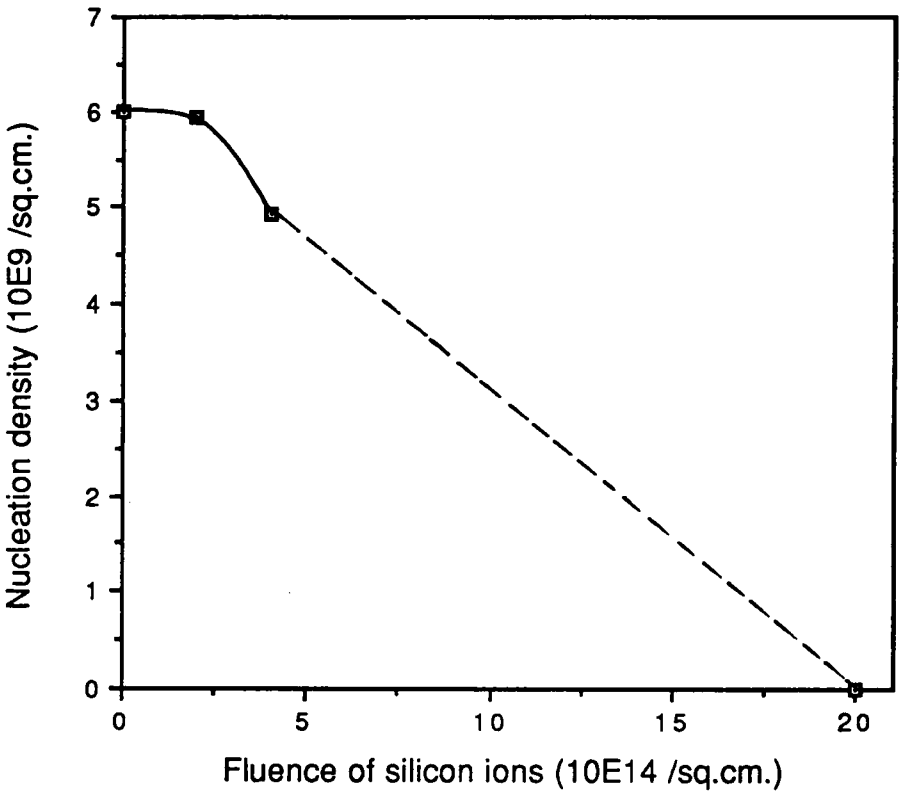


Figure 5.15. Effect of increasing fluence of Si ion implantation on the nucleation density of CVD diamond on Si faced 6H SiC

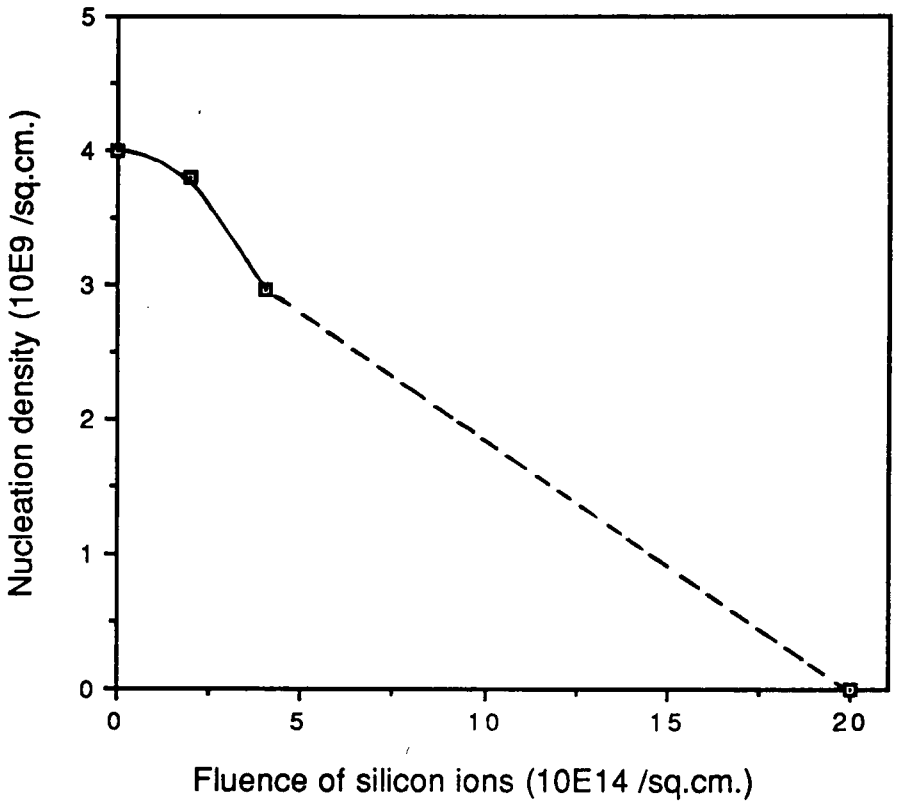


Figure 5.16. Effect of increasing fluence of Si ion implantation on the nucleation density of CVD diamond on C faced 6H SiC

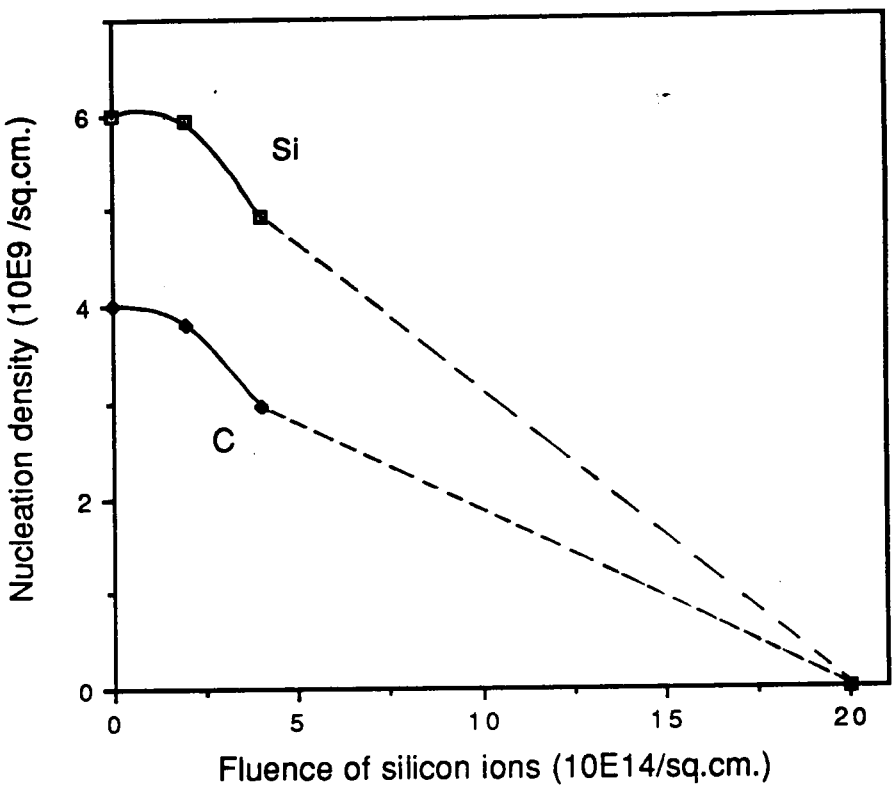


Figure 5.17. Carbon faced SiC has lower nucleation density in comparision to Si faced SiC substrates.

of higher back scattered yield. Si peak would have a higher energy compared to a C peak. The position of the peaks indicate the position of the damaged layer and the height of the peaks determine the amount of damage. Extensive damage occurs at high fluences and an amorphous layer is formed.

Figures 5.18 and 5.19 present the results of channeling on 6H silicon carbide implanted with Si^{29} at 150 keV. The presence of a peak in all the three cases of implantation implies the presence of an amorphous layer. From Figure 5.18, it can be seen that a sub-surface amorphous layer exists at a dose of 2 x 10^{14} Si^{+}/ cm^2. However, increasing the fluence to 4 x 10^{14} Si^{+} / cm^2 creates an amorphous layer nearer the surface but not at the surface (Figure 5.19). At a fluence of 2 x 10^{15} Si^{+} / cm^2 , the surface of the silicon carbide substrate becomes amorphous as can be seen from Figure 5.18. This amorphous surface layer probably contributes to the complete suppression of diamond nucleation.

However, literature reports the existence of a silicon carbide layer between the silicon substrate and diamond [30]. Extensive TEM studies have indicated that this layer is amorphous [55]. But the results of this study seem to contradict the idea that this amorphous layer might contribute positively to the nucleation process.

Figure 5.20 shows the nucleation of diamond on the back side of an unabraded Si faced sample. The sample was placed in the CVD chamber with the unpolished back side of the crystal exposed to diamond nucleation. In comparison to other micrographs, it can be seen that the surface of the substrate is rough. This, to some extent, verifies the theory that nucleation occurs on prominent rough features of the substrate, such as might be expected from abrasion [45,46].

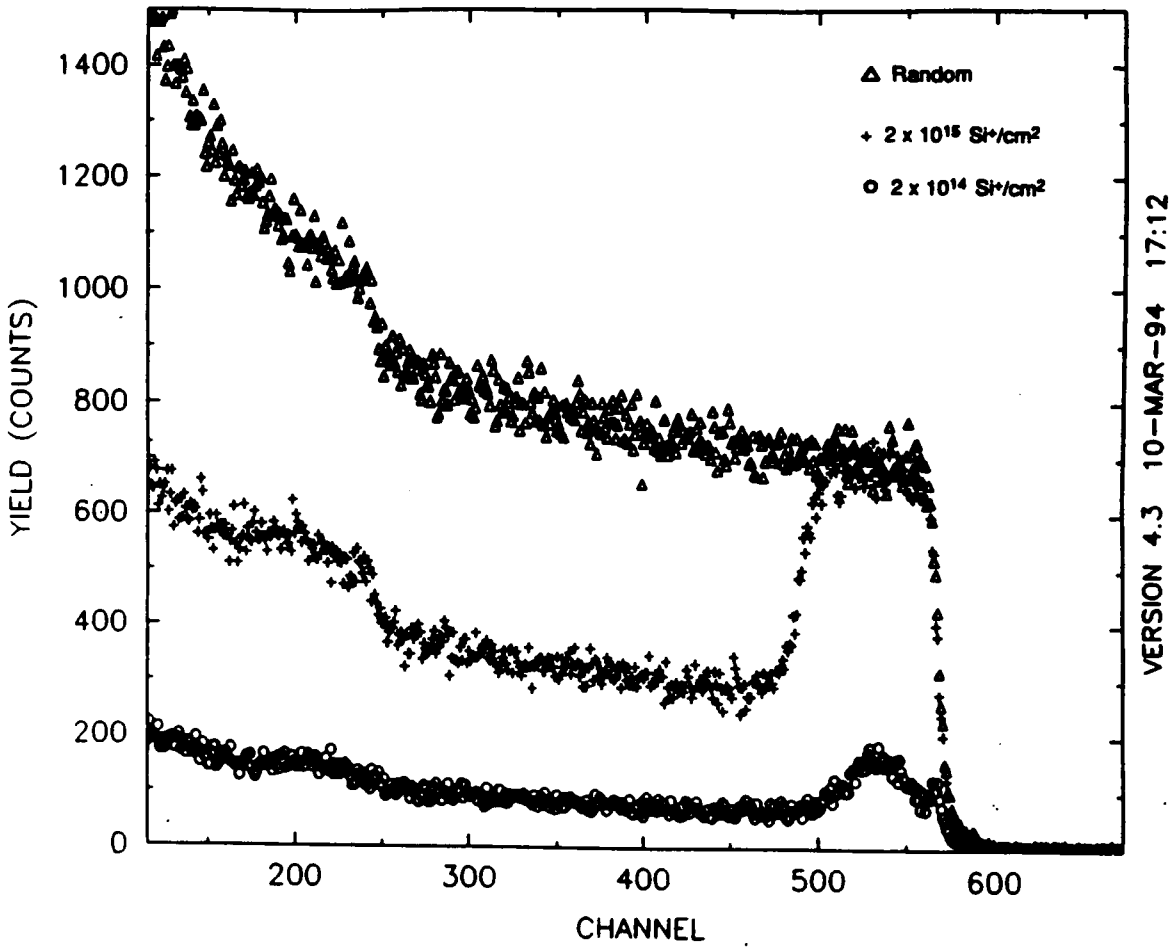


Figure 5.18. RBS/channeling of implanted 6H silicon carbide

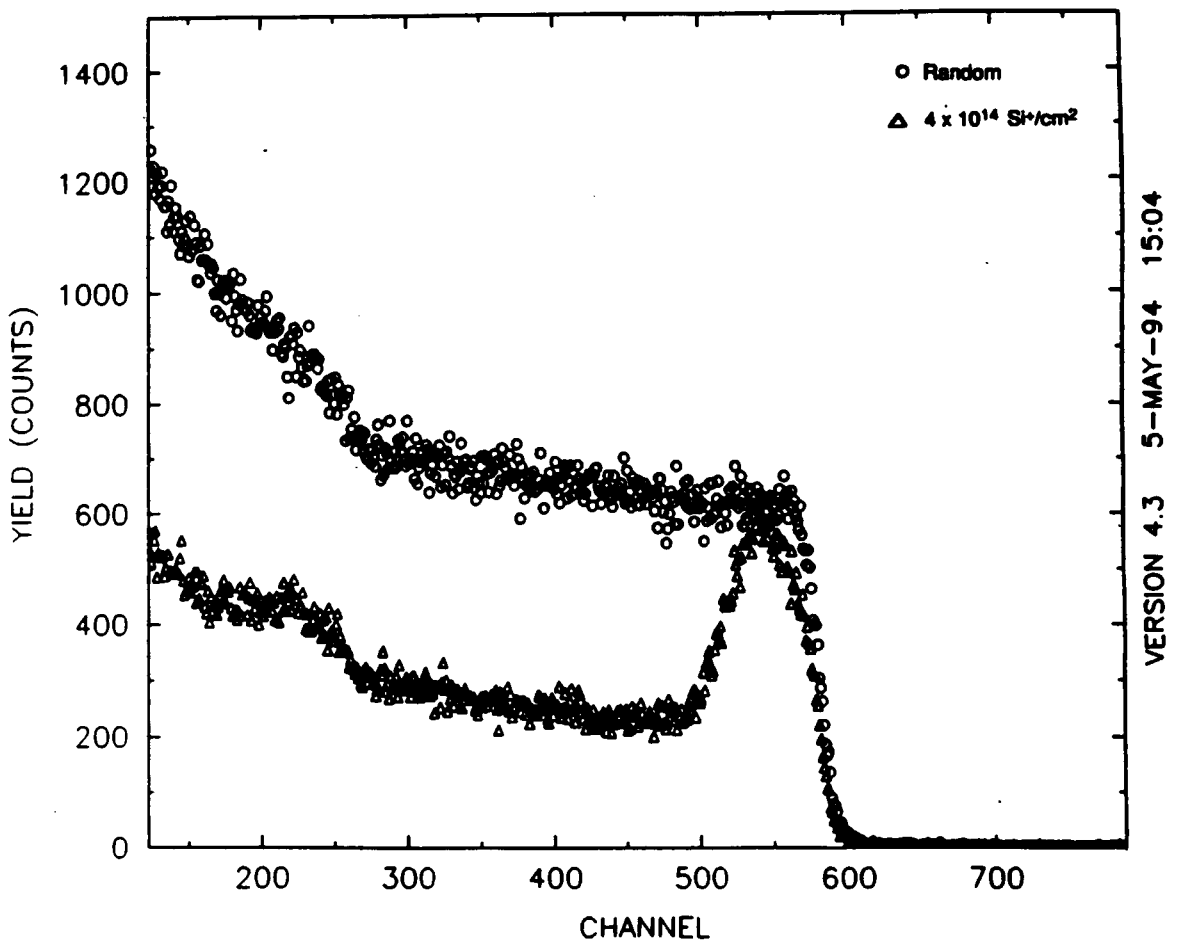


Figure 5.19. RBS/channeling of implanted 6H silicon carbide

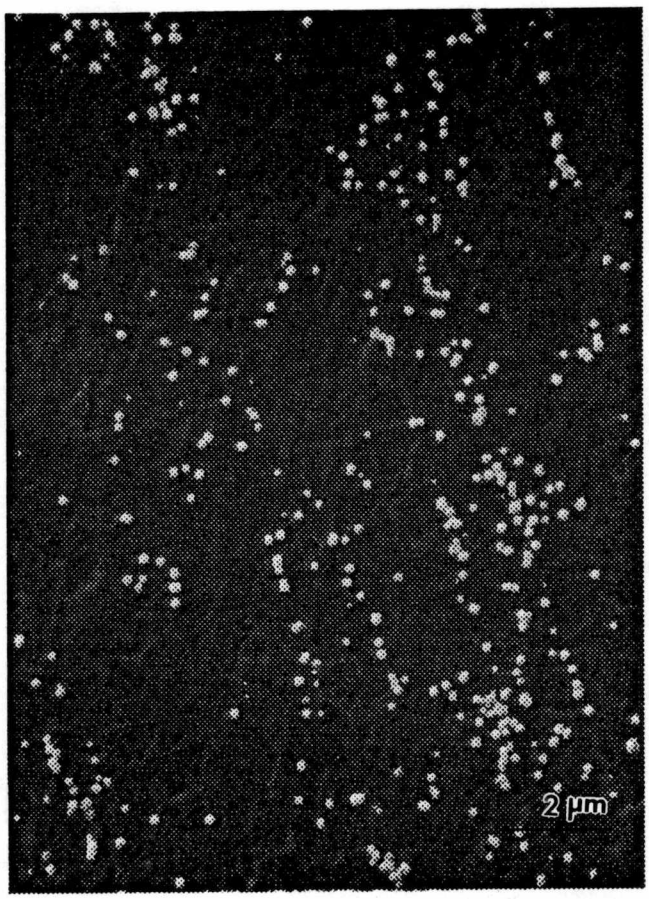


Figure 5.20. Scanning electron micrograph showing diamond nucleation on the back side of a silicon faced sample. The substrate surface is rough compared to the polished surfaces seen in other micrographs.

Hence, it is proposed that one of the reasons for the decrease in the nucleation density on implanted substrates could be the smoothing of microflaws during ion implantation.

CHAPTER 6
CONCLUSIONS

This study on the effect of surface defects on the nucleation of CVD diamond on 6H silicon carbide has enabled a better understanding of the mechanism of diamond nucleation. It is clear from this study that diamond does not nucleate on unabraded silicon carbide. The nucleation of diamond is greatly enhanced by abrasion of the silicon carbide surface with diamond powder prior to diamond deposition. This suggests that the surface damage/defects introduced by abrasion play a very important role in nucleation.

The fact that diamond did not nucleate on an amorphous silicon carbide surface contradicts the reports of the presence of an interfacial amorphous SiC layer between Si and diamond. The exact nature in which ion implantation effects the nucleation of diamond is not known. This study suggests that the decrease in nucleation density on ion implanted samples is a result of the smoothing of sharp features which were produced by diamond abrasion.

AFM (Atomic Force Microscopy) studies on the surface of abraded samples can be used to determine the nature of surface damage caused be abrasion. Also, a comparison with the surface characteristics of ion implanted samples can yield valuable information about the effect of ion implantation on the surface damage caused by abrasion.

Ion implantation can be used as a method for patterning of substrates for electronic applications. Substrates which were abraded with diamond in an ultrasonic vibrator can be implanted with high fluences of ions to create amorphous regions. Diamond growth on these samples will yield patterns with

diamond growth only in non implanted regions. This could be a very important technique once diamond semiconductors become a reality.

REFERENCES

LIST OF REFERENCES

1. M.W. Geis and J.C. Angus, *Scientific American*, October 92, p. 84
2. Zhidan Li, Doctoral Dissertation
3. J.C. Angus, in *Proceedings of First International Symposium on Diamond and Diamond-like Materials*, edited by J.P. Dismukes *et al.* (Electrochemical Society, Pennington, NJ,1989), p.1
4. F.P. Bundy, H.T. Hall, H.M. Strong, R.H. Wentorf, *Nature* **176**, (1955) 51
5. W. G. Eversole, U.S. Patent No. 3030188, Apr 17, 1962
6. J.C. Angus, H.A. Will, W.S. Stanko, J. Appl. Phys. **39**, (1968) 2915
7. J.C. Angus, N.C. Gardner, D.J. Poferl, S.P. Chauhan, T.J. Dyble and P. Sung, Sin. Almazy 3, (1971) 38; presented at the International Conference on Applications of Synthetic Diamonds in Industry, kiev, 1971
8. S.P. Chauhan, J.C. Angus and N.C. Gardner, J. Appl. Phys. **47** (1976) 4746
9. D.V. Fedoseev, S.P. Vnukov, B.V. Deryagin, Zh. Fiz. khimii, **51** (1977) 26
10. B.V.Spitsyn, 4th USSR Meeting Crystal Growth, Erevan University Publ. House, Ereven, (1972) 676-679
11. B.V. Spitsyn, L.L. Bouilov, and B.V. Derjaguin, J. Crystal Growth,**52** (1981) 219
12. B.V. Spitsyn and L.L. Bouilov, *Diamond and Diamond-Like Materials Synthesis*, April 1988, Ed. G.H. Johnson, A.R. Badzian and M.W. Geis, Mater. Res. soc., Pittsburgh (PA) (1988) 3-14

13. J.R. Wedlake, " Technology of Diamond Growth " in " The Properties of Diamond ", J.E. Field, editor, Academic Press, London, 1979, p 501-535
14. S. Matsumoto, Y. Sato, M. Kamo, and N. Setaka, Jpn. J. Appl. Phys., **21** (1982) 183
15. S. Matsumoto, Y. Sato, M. Tsutsumi, N.Setaka, J. Mat. Sci. **17** (1982) 3106
16. M. Kamo, Y. Sato, S. Matsumoto, S. Setaka, J. Cryst. Growth, **62** (1983) 642
17. T. A. Anthony, *Diamond and Diamond-Like Fims and Coatings*, Ed. R.E. Clausing, L.L. Horton, J.C. Angus and P. Koidl, Italy (1990) 555-577
18. I. Langmuir, J. Amer. Chem. Soc, **34** (1912) 860
19. I. Langmuir, J. Amer. Chem. Soc, **34** (1912) 1310
20. I. Langmuir and G.M.J. Mackay, J. Amer. Chem. Soc, **36** (1914) 1708
21. K.E. Spear, J. Am. Ceramic Soc., **72** (1989) 171
22. T.R. Anthony, MRS Fall Meeting, Nov 30-Dec 3 (1987) Boston
23. T.D. Moustakas, Solid State Ionics **32** (1989) 861
24. A. Sawabe and T. Inuzuka, Thin Soild Films **137** (1986) 89
25. J.E. Hughes, J. Less Common Metals,**1** (1959) 377
26. G.B. Gaines, C.T. Sims and R.I. Jaffe, J. Electrochem Soc, **106** (1959) 881
27. M. Yoshikawa, H. Ishida, A. Ishitani, T. Murakami, S. Koizumi and T. Inuzuka, Appl. Phys. Lett. **57** (1990) 428
28. B.E. Williams and J.T. Glass, J. mater. Res. 4 (1989) 373
29. J. Narayan, A.R. srivatsa, M. Peters, S. Yokota, and K.V. Ravi, Appl. Phys. lett. **53** (1988) 1823

30. D.G. Jeng, H.S. Tuan, R.F. Salat and G.J. Fricano, Appl. Phys. Lett. **56** (1990) 1968

31. Y. Sato, I. Yashima, H. Fujita, T. Ando, and M. Kamo, in *Proceedings of the Second International Comference on New Diamond Science and Technology*, edited by R. Messier, J.T. Glass, J.E. Butler, and R. Roy, MRS International Conference Proceedings (Materials Research Society, Pittsburgh, 1991) p. 371

32. B.V. Spitsyn, L.L. Bouilov, and B.V. Deryagin, J. Cryst. Growth **52** (1981) 219

33. X.K. Chen, G. Matera, S. Pramanick, and J. Narayan, in *Proceedings of the Second International Symposium on Diamond Materials*, edited by A.J. Purdes et al. (Electrochemical Society, Pennington, NJ, 1991), p.73

34. Y.H. Lee, K.J. Bachmann, J. T. Glass, Y.M. LeGrice, and R.J. Nemanich, Appl. Phys. Lett. **57** (1990) 1916

35. Y. Sato, I. Yashima, H. Fujita, T. Ando, and M. Kamo, *Second International Conference on New Diamond Science and Technology*, Washington, D.C., Sept. 23-27, 1990, edited by R. Messier, J.T. Glass, J.E. Butler, and R. Roy (Materials Research Society, Pittsburgh, 1991), p. 371

36. B.R. Stoner, G.-H.M. Ma, S.D. Wolter, and J.T. Glass, Phys. Rev. B **45** (1992) 11067

37. W. Zhu, X.H. Wang, B.R. Stoner, G.H. M. Ma, H.S. Kong, M.W.H. Braun, and J.T. Glass, Phys. Rev. B **47** (1993) 6529

38. J.L. Robins, Appl. Surf. Sci. **33/34**, (1988) 379

39. P.K. Bachmann, W. Drawl, D. Knight, R. Weimer, and R.F. Messier, in *Diamond and Diamond-Like Materials Synthesis,* edited by G.H. Johnson, A.R. Badzian, and M.W. Geis (Materials Research Society, Pittsburgh, 1988) p. 99.

40. S. Iijima, Y. Aikawa, and K. Baba, Appl. Phys. Lett. **57** (1990) 2646

41. S. Iijima, Y. Aikawa, and K. Baba, J. Mater. Res. **6** (1991) 1491

42. K. Suzuki, A. Sawabe, H. Yasuda, and T. Inuzaka, Appl. Phys. Lett. **50** (1987) 728

43. A. Sawabe and T. Inuzula, Thin Solid Films **137** (1986) 89

44. C. P. Chang, D.L. Flamm, D.E. Ibbotson, and J.A. Mucha, J. Appl. Phys. **63** (1988) 1744

45. P.A. Dennig and D.A. Stevenson, in *Proceedings of the Second International Conference on the New Diamond Science and Technology,* edited by R. Messier and J.T. Glass (Japan New Diamond Forum, Washington D.C., 1990)

46. P.A. Dennig and D.A. Stevenson, in *Proceedings of the First International Conference on the Applications of Diamond Films and Related Materials,* edited by Y. Tzeng, M. Yoshikawa, M. Murakawa, and A. Feldman (Elsevier, New York, 1991), p. 383

47. S. Yugo, A. Izumi, T. Kanai. T. Muto, and T. Kimura, *Second International Conference on New Diamond Science and Technology,* Washington, D.C., Sept. 23-27, 1990, edited by R. Messier, J.T. Glass, J.E. Butler, and R. Roy (Materials Research Society, Pittsburgh, 1991), p. 385

48. R.J. Meilunas, R.P. Chang, S. Liu, and M.M. Kappes, Appl. Phys. Lett. **59** (1991) 3461

49. K.V. Ravi and C.A. Koch, Appl. Phys. Lett. **57** (1990) 348

50. K.V. Ravi, C.A. Koch, H.S. Hu, and A. Joshi, J. Mater. Res. **5** (1990) 2356

51. A.A. Morrish and P.E. Pehrsson, Appl. Phys. Lett. **59** (1991) 417

52. B.R. Stoner and J.T. Glass, Appl. Phys. Lett. **60** (1992) 698

53. B.R. Stoner, S.R. Sahaida, J.P. Bade, P. Southworth, and P.J. Ellis, J. Mater. Res. **8** (1993) 1334

54. B.R. Stoner, G.H. Ma, S. D. Wolter, W. Zhu, Y. C. Wang, R.F. Davis and J.T. Glass, Diamond and Related Materials, **2** (1993) 142

55. B.E. Williams and J.T. Glass, J. Mater. Res. **4** (1989) 373

56. P.O. Joffreau, R. Haubner, and B. Lux, Int. J. Refract. Hard Met. December (1988) 186

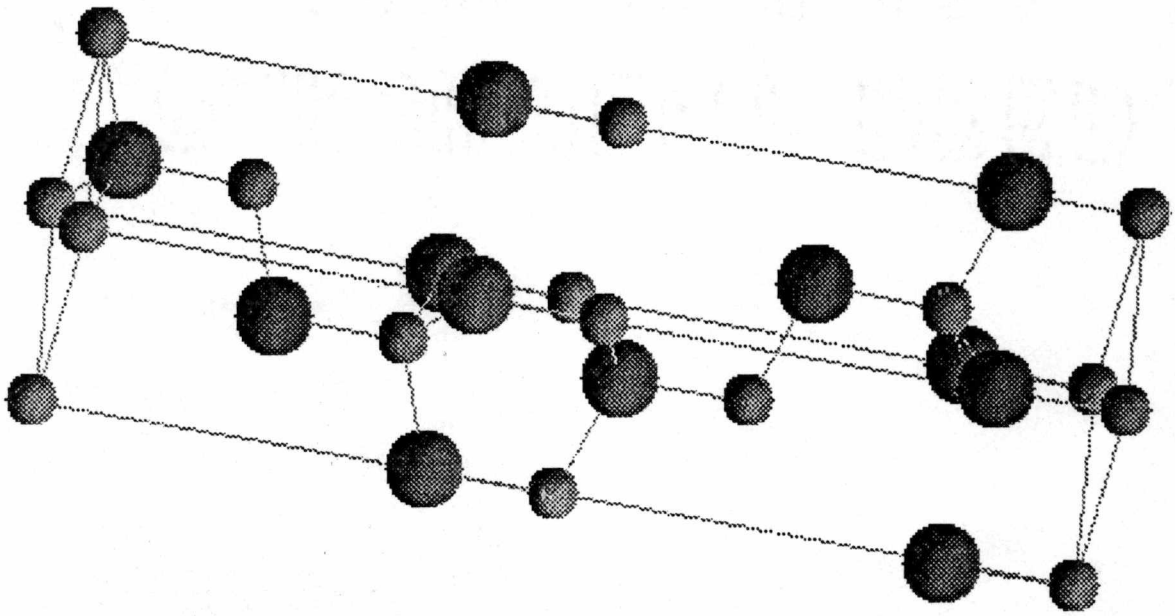
57. J.J. Dubray, C.G. Pantano, M. Meloncelli, and E. Bertran, J. Vac. Sci. Technol. A **9** (1991) 3012

58. T. Hartnett, R. Miller, D. Montanari, C. Willingham, and R. Tustison, J. Vac. Sci. Technol. A **8** (1990) 2129

59. C.J. McHargue, M.B. Lewis, B.R. Appleton, H. Naramoto, C.W. White, and J.M. Williams, in *Science of Hard Metals*, edited by R.K. Viswanadham, D.J. Rowcliffe, and J. Gurland (Plenum, New York, 1983) p. 451

60. P.J. Burnett, T.F. Page, J. Mater. Sci. **19**, (1984) 3524

APPENDIX



Crystal structure of 6H silicon carbide

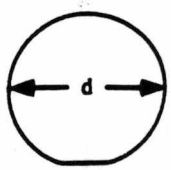
CREE

The Leader in Silicon Carbide Solid State Technology

6H Silicon Carbide
Material Data Sheet

Physical Properties§

Polytype:	Single Crystal 6H
Crystal Structure:	Hexagonal
Band Gap:	2.9 eV
Thermal Conductivity:	4.9 W/cm • K
Lattice Parameters:	a = 3.08 Å c = 15.12 Å
Mohs Hardness:	9



d = 1.0 inch +/- 0.020
Orientation of wafer flat
$<11\bar{2}0>$ +/- 10°

Substrate Specification

Diameter:	1 inch +/- 0.020
Thickness:	0.013 inches (+/- 0.005 inches)
Conductivity Type:	n or p
Net Doping Density:	n-type selection range: 3×10^{17} - 2×10^{18}/cm^3 (N_D-N_A) n-type tolerance: +/- a factor of 2 p-type selection range: 7×10^{17} - 3×10^{18}/cm^3 (N_A-N_D) p-type tolerance: +/- a factor of 2
Wafer Orientation:	On Axis: {0001} +/- 0.5° Off Axis: 3.5° +/- 0.5° Off {0001} toward <1120> +/- 10°
Polished Side:	Silicon or Carbon Face

Epitaxial Specification*

Net Doping Density:	n-type selection range: 2×10^{16} - 5×10^{18} /cm^3 (N_D-N_A) p-type selection range: 2×10^{16} - 1×10^{18} /cm^3 (N_A-N_D) tolerance: specific to order
Thickness‡:	selection range 0.20 - 10.0 microns tolerance: +/- 40% of selected thickness

VITA

Sunil Abraham was born in Kerala, India on July 28, 1970. After graduating from Vyomayana Samastha Vidyalaya, Orissa in June 1988, he entered the Indian Institute of Technology, Kharagpur. He received a B.Tech (Honors) in Metallurgical engineering in July 1992.

In August 1992, he accepted a position at Essar Steel in Gujarat, India. In January 1993, he joined the University of Tennessee to pursue a M.S. in Materials Science and Engineering.

He is a member of the ASM International and the Metals, Minerals and Materials Society.